HYDROTHERMAL-LIKE SYNTHESIS OF HYDROXYAPATITE FROM CALCIUM SULFATES

A THESIS SUBMITTED TO
THE GRADUATE SCHOOL OF NATURAL AND APPLIED SCIENCES
OF
MIDDLE EAST TECHNICAL UNIVERSITY

BY

ONUR RAUF BİNGÖL

IN PARTIAL FULFILLMENT OF THE REQUIREMENTS
FOR
THE DEGREE OF MASTER OF SCIENCE
IN
METALLURGICAL AND MATERIALS ENGINEERING

SEPTEMBER 2010

Approval of the thesis:

HYDROTHERMAL-LIKE SYNTHESIS OF HYDROXYAPATITE FROM CALCIUM SULFATES

submitted by **ONUR RAUF BİNGÖL** in partial fulfillment of the requirements for the degree of **Master of Science in Metallurgical and Materials Engineering, Middle East Technical University** by

Prof. Dr. Canan Özgen
Dean, Graduate School of **Natural and Applied Sciences** _____

Prof. Dr. Tayfur Öztürk
Head of Department, **Metallurgical and Materials Engineering** _____

Assoc. Prof. Dr. Caner Durucan
Supervisor, **Metallurgical and Materials Engineering Dept., METU** _____

Examining Committee Members:

Prof. Dr. Tayfur Öztürk
Metallurgical and Materials Engineering Dept., METU _____

Assoc. Prof. Dr. Caner Durucan
Metallurgical and Materials Engineering Dept., METU _____

Prof. Dr. Amdulla O. Mekhrabov
Metallurgical and Materials Engineering Dept., METU _____

Assist. Prof. Dr. Dilek Keskin
Deparment of Engineering Sciences, METU _____

Assist. Prof. Dr. H. Emrah Ünalan
Metallurgical and Materials Engineering Dept., METU _____

Date: 07.09.2010

I hereby declare that all information in this document has been obtained and presented in accordance with academic rules and ethical conduct. I also declare that, as required by these rules and conduct, I have fully cited and referenced all material and results that are not original to this work.

Name, Last Name : ONUR RAUF BİNGÖL

Signature :

ABSTRACT

HYDROTHERMAL-LIKE SYNTHESIS OF HYDROXYAPATITE FROM CALCIUM SULFATES

Bingöl, Onur Rauf
M.Sci., Department of Metallurgical and Materials Engineering
Supervisor: Assoc. Prof. Dr. Caner Durucan

September 2010, 80 pages

Synthesis of hydroxyapatite ($Ca_{10}(PO_4)_6(OH)_2$, HAp) from commercial grade plaster of paris ($CaSO_4 \cdot 0.5H_2O$, PoP) and gypsum ($CaSO_4 \cdot 2H_2O$) has been performed. HAp synthesis was achieved by reacting 1 M of $(NH_4)_2HPO_4$ (or 0.5 M of $(NH_4)_2HPO_4$) solutions with solid calcium sulfate precursors under ambient pressure (1 atm) and hydrothermal-like (2 ± 0.2 atm, 120 °C) conditions. Under ambient conditions, HAp formation kinetics was investigated at 25 °C, 50 °C and 90 °C using 1 M of $(NH_4)_2HPO_4$ solution. Conversion to HAp at such low temperature takes more than 21 days and it also promotes formation of additional calcium phosphate with HAp. At 25 °C, HAp formation started after 7 days accompanied with formation of brushite ($CaHPO_4 \cdot 2H_2O$). At 50 °C no significant conversion was observed after 6 h. However, at 90 °C, phase pure HAp was formed after 2 h. On the other hand, under hydrothermal-like conditions, the HAp formation proceed much faster and it was also shown that HAp could be also synthesized from gypsum powders and bulk gypsum pellets. Using 1 M of

$(NH_4)_2HPO_4$ solution, HAp formation from PoP started 15 min and completed almost in 30 min, whereas 0.5 M of $(NH_4)_2HPO_4$ reactant solution slowed down the conversion. The exact chemical identity of the HAp product of hydrothermal-like reaction was evaluated by post-synthesis calcinations and the thermal phase stability was related with the stoichiometry (Ca/P at ratio) of the HAp. The HAp phase was stable up to 600 °C and above 600 °C, β-tricalcium phosphate (β-$Ca_3(PO_4)_2$, β-TCP) was formed, suggesting that the resultant HAp was calcium-deficient. Mechanical testing by diametrical compression was performed to the HAp samples produced from bulk gypsum pellets. The strength was measured 1.2 MPa with highest solid to liquid (*s:l*) ratio 3.33 and decreased with *s:l* ratio. This change was found to be related with the porosity differences due to differences in *s:l* ratio. Additional mechanical tests were applied to the polycaprolactone (PCL) coated bulk HAp pellets for which the tensile strength was doubled. This study presents an easy and feasible method for production of HAp from a cheap and abundant calcium source – PoP. In addition, the findings provide a potential processing route for developing irregularly shaped bulk porous HAp structures.

Keywords: Hydroxyapatite, calcium phosphates, calcium sulfate, powder synthesis, hydrothermal synthesis

ÖZ

KALSİYUM SÜLFATLARDAN HİDROTERMAL BENZERİ METODLAR İLE HİDROKSİAPATİT SENTEZLENMESİ

Bingöl, Onur Rauf
Yüksek Lisans, Metalurji ve Malzeme Mühendisliği Bölümü
Tez Yöneticisi: Doç. Dr. Caner Durucan

Eylül 2010, 80 sayfa

Bu çalışmada, ticari saflıkta alçı ($CaSO_4 \cdot 0.5H_2O$) ve su ile sertleştirilmiş alçıtaşı ($CaSO_4 \cdot 2H_2O$) kullanılarak hidroksiapatit ($Ca_{10}(PO_4)_6(OH)_2$, HAp) sentezlendi. HAp sentezi farklı sıcaklıklarda atmosferik (1 atm) ve hidrotermal-benzeri (2 ± 0.2 atm) koşullarda 1 M ve 0.5 M $(NH_4)_2HPO_4$ çözeltileri kullanılarak gerçekleştirildi. Atmosferik koşullarda HAp, 1 M'lık $(NH_4)_2HPO_4$ çözeltisi kullanılarak 25 °C, 50 °C ve 90 °C'de sentezlendi. Düşük sıcaklıklar HAp oluşum süresini 21 güne kadar uzatırken ve farklı kalsiyum fosfat fazlarının oluşumunu da tetikledi. 25 °C'de 7 gün sonunda HAp'e ek olarak farklı bir kalsiyum sülfat fazı – bruşit ($CaHPO_4 \cdot 2H_2O$) oluşumu gözlemlenirken, 50 °C'de 6 saate kadar yapılan çalışmalarda HAp oluşmadığı tespit edildi. Ancak, 90 °C'de 2 saat sonunda HAp oluşumu gözlendi. Buna karşılık, hidrotermal-benzeri koşullarda çok daha kısa sürede hem toz alçı hem de katı alçıtaşından HAp üretilebileceği gösterildi. 1 M $(NH_4)_2HPO_4$ çözeltisi kullanılarak hidrotermal-benzeri koşullarda 120 °C'de 15 dakikada HAp dönüşümünün başladığı ve 30 dakika içinde büyük ölçüde

dönüşümün tamamlandığı gözlemlendi. Diğer taraftan, 0.5 M $(NH_4)_2HPO_4$ çözeltisinin kullanımı dönüşüm kinetiğini düşürdüğü tespit edildi. Hidrotermal-benzeri koşullarda üretilen HAp tozlarının kesin kimsayal özelliği üretim sonrası kalsinasyonlar ve x-ışınları kırınım (XRD) analizleri yardımı ile tespit edildi. Termal kararlılığının kimyasal komposizyon (Ca/P oranı) ile ilgili olduğu saptandı. Oluşan HAp'in 600 °C'ye kadar kararlı olmasına rağmen 600 °C üzeri sıcaklıklarda, β-trikalsiyum fosfat (β-$Ca_3(PO_4)_2$, β-TCP) fazına dönüştüğü görüldü. Bu tespit, oluşan HAp'in kesin bileşimli (stoichiometric) HAp'a göre daha düşük miktarda kalsiyum içerdiğini göstermektedir. Hidrotermal-benzeri metodlar ile alçıtaşıdan HAp'e dönüştürülen katı yapıların mekanik dayançları diametrik basma testi ile ölçüldü. En yüksek katı:sıvı oranına (3.33) sahip olan katı örneklerin dayancı 1.2 MPa olarak gözlemlendi ve dayancın katı:sıvı oranına bağlı olduğu saptandı. Ek olarak, polykaprolakton (PCL) ile kaplanmış HAp yapılarının mekanik dayancı incelendi ve kaplama sonrasında dayancın iki katına çıktığı gözlemlendi. Bu çalışma sonucunda endüstriyel üretim süreçlerine uyarlanabilecek bir metod ile ucuz bir kalsium kaynağından HAp sentezlenebileceği ortaya konuldu. Bunun yanında, söz konusu üretim süreci, farklı şekillerde gözenekli katı HAp seramik yapılarının üretimini mümkün kılmaktadır.

Anahtar kelimeler: Hidroksiapatit, kalsiyum fosfatlar, kalsiyum sülfat, toz sentezi, hidrotermal sentez

To my family...

ACKNOWLEDGEMENTS

I sincerely acknowledge Assoc. Prof. Dr. Caner Durucan for his authentic support and unique guidance. I could not get through this task without his help and comments.

I would like to thank Serkan Yılmaz and Hülya Yalçın for their help in SEM analyses and Necmi Avcı for XRD analyses.

I owe my deepest gratitude to my teammates – Betül Akköprü, Özlem Altıntaş Yıldırım, Tümerkan Kesim, Hakan Yavaş, Gülçin Çiçek and Özgecan Dervişoğlu. I will never forget the chats, laughs, discussions; besides, their precious support and help during this period.

I also would like to show my gratitude to Hüseyin Ergün, Sadık Bayramoğlu, Serdar Savaş, Göksu Gürer, Alp Aykut Kibar, Murat Tolga Ertürk and Emre Topsoy for their kindness and infinite support. Their friendship and positive attitudes along my graduate and undergraduate life are priceless.

And… my mom and dad… It is impossible to express my feelings by any known words about your support, friendship and guidance throughout my life. Your love is the most valuable thing I have ever had. Thank you for everything….

TABLE OF CONTENTS

LIST OF FIGURES

FIGURES

LIST OF TABLES

TABLES

CHAPTER 1

INTRODUCTION AND LITERATURE REVIEW

1.1. General introduction of the thesis

For many years people have developed various devices to fix broken bones and fill the bone defects. These devices include metallic, ceramic and polymeric implants and their composites. The main challenge in developing these devices is to achieve maximum biocompatibility and maximum integration capability with the bone. Metal alloys, such as stainless steel, cobalt-chromium and titanium alloys, are the most common ones, especially on load-bearing applications. However; they are not biocompatible, they do not integrate with bone and they cause stress shielding, i.e. reduction in bone strength due to removal of the load from bone by the implant. Another choice is polymeric materials such as polymethylmetacrylate (PMMA). They have high strength, which allows them to be used in load-bearing applications; however, they are not resistant to creep, they have low modulus and essentially, they may dissolve in physiological environment and generate toxic monomers. Due to the toxicity of these types of polymers, more biocompatible choices are produced, such as polylactic acid (PLA) and polyglycolic acid (PGA). The main advantage of these materials is their biodegradable (dissolve into H_2O and biomolecules in physiological environment) nature, however; they have low strength and consists of the drawbacks of the polymeric materials.

In biomedical applications, ceramic materials have an important place. The first generation of ceramic materials (i.e. alumina (Al_2O_3), yttria-stabilized zirconia (Y-TZP)) has superior mechanical properties (strength and hardness), however they

are bioinert. They do not react with the body, but they do not harm the body either. Nevertheless, the modern research has turned into bioactive ceramics, especially calcium phosphate ceramics. The most important one in calcium phosphate ceramics area is hydroxyapatite ($Ca_{10}(PO_4)_6(OH)_2$, HAp). HAp has the same constituents of the bone mineral and it has similar chemical structure and behavior compared to bone mineral. This makes calcium phosphate ceramics, and mainly HAp, highly biocompatible and bioactive, allowing tissue attachment and ingrowth on the implant.

In production of HAp, calcium salts, calcium carbonate ($CaCO_3$) and calcium oxide (CaO) are generally used as starting materials. Recently, calcium sulfate ($CaSO_4$) has gained attention as a starting material to synthesize HAp. Calcium sulfate has high availability and relatively low cost compared to other starting materials. In addition to those, calcium sulfate, on its own, is highly biocompatible and bioactive as well as high absorption rate by the physiological environment.

It is possible to synthesize HAp powders by several methods, such as wet chemical, solid state and hydrothermal methods. Solid state method is the conventional method to produce various ceramic powders and also HAp powders. The main disadvantage of this method is the need of high firing temperatures and long reaction times in order to prevent any chemical and microstructural inhomogeneity in the products. Wet chemical methods are relatively easy to conduct and, therefore; it is frequently used. They need relatively low temperatures and they are as simple as mixing the solution to precipitate HAp particles. However, the products are poorly crystallized, inhomogeneous in composition and irregularly shaped. Additionally, solvent removal processes cause inhomogeneities even if the starting solution is homogeneous. Hydrothermal methods combine relatively high temperatures compared to wet chemical methods with high pressure. The pressure allows boiling the aqueous solutions at higher temperatures than their equilibrium boiling temperature. Hydrothermal reactions generate highly homogeneous crystal products. The shape and size of the crystals can be also controlled. As a result, hydrothermal synthesis methods allow superior control on the morphology, composition and powder reactivity.

The controlled synthesis of the HAp powders enables better control on their mechanical strength. Nonetheless, the mechanical properties bulk ceramic HAps are poor compared to alumina and Y-TZP. A common method to increase their mechanical strength is coating with biodegradable polymers. Several biodegradable polymers, such as PLA, PGA and polycaprolactone (PCL) can be coated on HAp scaffolds and making them ceramic/polymer composites.

In this thesis, chemical, physical and morphological properties of commercial grade plaster of paris ($CaSO_4 \cdot 0.5H_2O$) and its hydrated from, gypsum ($CaSO_4 \cdot 2H_2O$) were investigated. Moreover, the conversion kinetics of the calcium sulfate to HAp reaction by hydrothermal-like conditions and the morphology of the HAp product were also examined systematically. Finally, the exact chemical identity and the mechanical properties of the HAp product, which is converted from gypsum, have been investigated.

1.2. Background information and literature review

1.2.1. Bone: Chemical, structural and mechanical properties

Bone is structurally a composite material mainly consisting of a mineral phase (calcium phosphate, 69 wt. %), an organic phase (collagen, 20 wt.%) and water (9 wt.%). In addition, several organic materials, such as proteins, polysaccharides and lipids, are included in small quantities [1].

The main organic phase, collagen, can be called as the matrix of the composite bone material [1]. They are characterized by the fibrils having a diameter about 80-10 nm. Each fibril is constructed from three polypeptide chains about 1000 amino acids long and they are connected to each other in a triple helix. The organic phase also includes blood vessels. A representative schematic illustration of bone is provided in Figure 1.1. The water inside the bone is placed inside the fibril, the gaps and between the triple-helical molecules [2]. The mineral phase, calcium phosphate, presents in the form of apatite which is the main mineral component of the bone and tooth. This apatitic calcium bone mineral is similar to a synthetic apatite, hydroxyapatite ($Ca_{10}(PO_4)_6(OH)_2$, HAp), however; it differs from HAp in stoichiometry (Ca/P ratio), morphology and crystal size. The biological apatite has lower Ca/P ratio compared to the synthetic counterpart (which has a Ca/P ratio of 1.67) and it presents as a carbonated form in nature [3, 4]. The biological apatite phase has a structure composed of nano-crystalized plates or needles and also, this phase exists as a continuous phase deposited parallel to the collagen fibrils in the bone [1]. The synthetic HAp can also be present in different crystal sizes and morphologies depending mainly on the synthesis method.

The human bone mainly consists of two types: cancellous (spongy) and cortical (compact). The cancellous bone is mainly located on the ends of the long bones, i.e. femur, in addition to the flat, short and irregular bones. It has high porosity, i.e. 50 - 90 vol%. The compact bone is located mainly in the middle of the long bones and it has lower porosity, i.e. 5 – 10 vol%. The porosity also affects the mechanical properties in addition to the age (mineralization), constituents of the bone, collagen orientation and the load direction. Due to these reasons, the bone

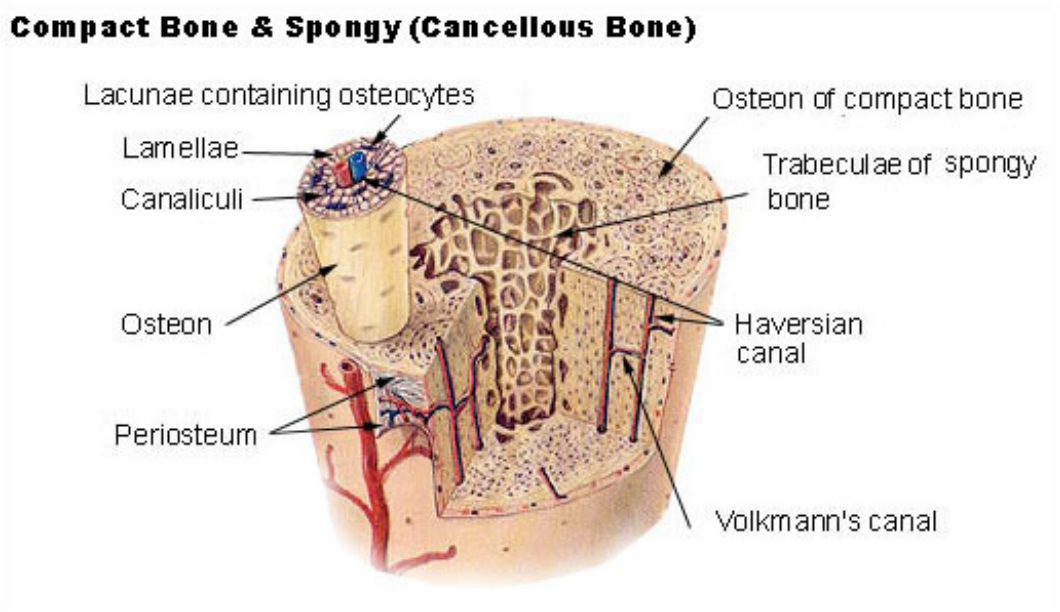

Figure 1.1 Schematic representation of bone showing its organic and mineral phases [5]

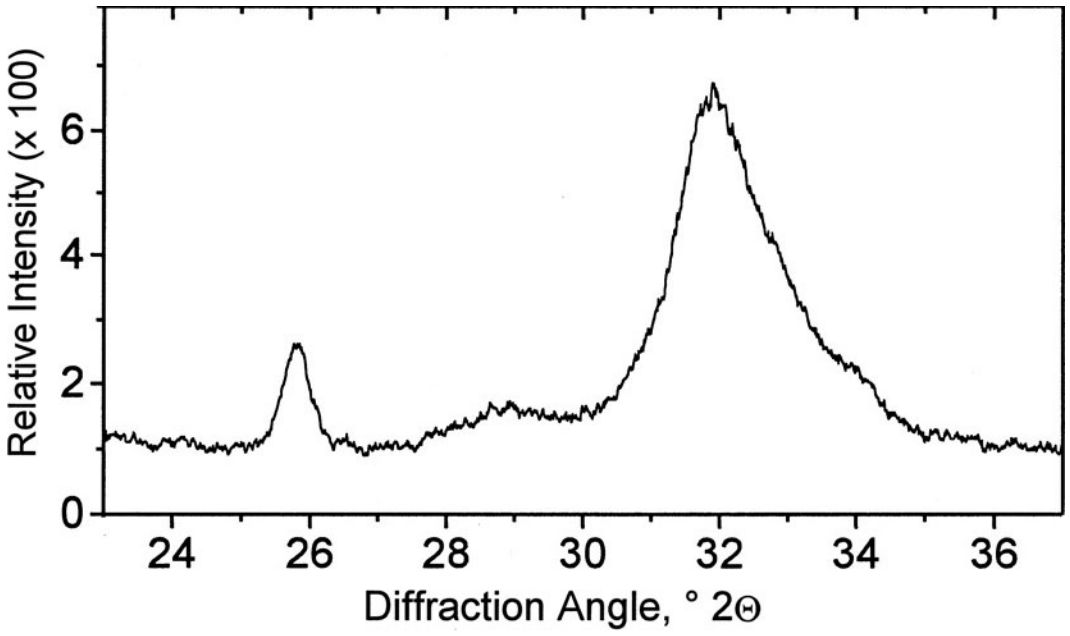

Figure 1.2 XRD diffractogram of human bone [6]

may fracture and it should be repaired internally or externally by a kind of implant produced from natural bone or synthetic bone-like materials.

1.2.2. Synthetic analogs for filling bone defects

Throughout the years, people have used several types of prostheses and implants in order to heal the fractures of the bone and to replace defective bone tissue. Stainless steel, cobalt-chromium alloys and titanium alloys have been used for this purpose. The metal implants have good toughness and strength, and they are still used in fixation of the bones in load-bearing applications. However, the metal implants are biologically inert and not biocompatible [7]. They are not biocompatible, they cause stress shielding in the bone, and they do not combine the main properties of the ideal bone replacement material, i.e. osteoconduction (the ability to form and connect to the continuous layer of bone with chemical bonding), osteointegration (the ability to support the bone growth on its surface), osteoinduction (the ability to create living tissues on the implant) and osteogenesis (the ability to form osteblastic cells within the implant).

According to these factors, the main idea behind a replacement material for the bone is to produce a bone-like material having same chemical and mechanical properties or to use natural bone grafts. Therefore, calcium phosphates are used and their usage is mainly focused on HAp due to the high biocompatibility and capability of osteointegration and osteoconduction. However, calcium phosphates or real bone replacements are ceramics and ceramics are known as their poor toughness. As a result, it is impossible to use them on load-bearing applications.

According to Moore et. al., replacements for the local loss of the bones are important in biomedical applications [8]. This phenomenon brings up the factor of filling the irregular defects of the bone. Filling irregular defects in bone allows perfect osteointegration, osteoconduction, osteoinduction and osteogenesis conditions addition to high biocompatibility and high mechanical properties (without causing any stress shielding) in non-load bearing applications. Metal implants are not suitable for filling irregular defects of the bone, whereas ceramic or polymeric implants and the bone itself are better choices.

1.2.2.1. Natural bone grafts

In biomedical and clinical applications, there are three concepts of natural bone grafts: xenograft, allograft, autograft. Xenografts are obtained from animal bones, i.e. bovine bones. They are only osteoconductive. However, xenograft implantations cause viral infections in human body [9]. Allograft is an alternative to xenograft implants. It is derived from the bones from the same species which the prosthesis was implanted. It has osteoconductive and osteoinductive properties, however; it is not osteogenic because it does not contain any living component. Autograft is the best alternative in this group. It is derived from the same individual to whom the prosthesis was implanted. It has all of the main properties: osteointegration, osteocondition, osteoinduction and osteogenesis [8, 9]. Additionally, it is the most compromising bone graft in this group.

1.2.2.2. Natural materials

The usage of the natural organisms is the first approach to repair bone defects. In 1972, it was found that a missing tooth is replaced by nacre substitutes in Mayan skulls about 4000 years old. Nacre is a natural composite having nearly 95 wt% of aragonite (calcium carbonate) phase and 5 wt% of organic phase (proteins, polysaccharides) [10]. This approach is not common in today's practice.

1.2.2.3. Inert ceramics

Biologically inert ceramic materials, i.e. alumina (Al_2O_3) and zirconia (as yttria-stabilized tetragonal zirconia polycrystal, Y-TZP) were the firstly employed synthetic porous scaffolds for filling bone defects in biomedical industry. These ceramics can be produced only in certain chemical composition and the mechanical and the biological properties directly affected by the composition of the ceramic material. Because they are biologically inert, they do not integrate with the bone tissue. Although these ceramics do not form chemical bonding between the bone tissues, a mechanical bond forms between the implant and the bone tissue due to the applied stresses on the affected bone [11]. However, this

Figure 1.3 An optical image of porous alumina ceramic [12]

mechanical bonding causes stress shielding and, therefore; bioinert ceramics are hardly used as bone fillers.

Alumina has been used, firstly, for hip prostheses due to its low friction and wear coefficients. This makes the alumina resistant to wear and corrosion. However, alumina lacks for its low mechanical properties. In 1990's, Y-TZP has become popular for its high fracture toughness and strength in a ceramic material for medical use. In addition to the high strength values, it has extremely low wear rates compared to alumina [11]. Stabilization property has increased crack propagation resistance by transformation of the phases (i.e., transformation toughening). This transformation creates metastable phases and these phases cause Y-TZP to degrade in presence of water. As a result, more stable and stronger ceramics are in need in today's medical arena.

1.2.2.4. Bioactive glasses and glass ceramics

Roots of using glasses in bone defects go back to 1969. As defined in 1969, the bioactive glasses (bioglasses) are hard and non-porous materials. They are made of sodium oxide, calcium oxide, phosphorus pentaoxide and the main constituent, silica. The solubility and fixation capability, which is the main advantage of bioactive glass, is controlled by the variation in the composition of the glass in addition to good osteointegrative and osteoconductive properties. The main disadvantage is low mechanical properties and impossibility to use in load-bearing applications [13].

The principle behind good osteointegrative and osteoconductive properties is the strong chemical bonding between the bone and the bioglass. This bonding forms a silica-rich gel layer due to the effect of the interaction between the bioglass and the physiologic aqueous solutions on the connection surface. In the gel layer, calcium and phosphate ions combine to form HAp, with higher mechanical properties compared to ceramic HAp [8].

Previous studies show that it is possible to increase the mechanical properties of the bioglass in a specific chemical composition by precipitation of β-wollastonite ($CaO \cdot SiO_2$) and oxyfluoroapatite ($Ca_{10}(PO_4)_6(O,F_2)$) in the amorphous glass matrix resulting apatite/wollastone (A/W) glass ceramic [14]. However, the increase in the mechanical properties is much higher than the cortical bone [8].

Recent trend on bioglass technology is forming bioglass composites with polymers. The mechanical properties of such composites are found to be close to that for the cortical bone [8]. This type of composites are mainly used in dental implants [15].

1.2.2.5. Polymers and polymer-composites

Polymers are widely used in clinical applications since 1960. At first, the main focus was on the bone cements. Acrylic bone cements are the first utilized polymeric materials to fix the broken bones. Polymethylmethacrylate (PMMA) is also bone cement and it is still used as bone cement in today's clinical applications. PMMA is excellent to fix prostheses mechanically but it does not allow biological fixation. [11]. PMMA sets by polymerizing toxic raw materials with highly exothermic reaction which causes bone deformation and infections. PMMA also does not degrade in physiological environment, and therefore; it is not bioactive and biocompatible [9]. Nonetheless, the most popular polymeric materials in biomedical industry are biodegradable polymers, such as polylactic acid (PLA), polyglycolic acid (PGA) and their co-polymers, poly(lactic-co-glycolic) acid (PLGA). They are highly biocompatible, osteoconductive and osteointegrative. In addition to these polymers, polycaprolactone (PCL) and polymers having biological origin such as starch, chitosan, gelatin, collagen, silk

Figure 1.4 An optical image of Immix Extenders (Osteobiologics, Inc.), a particulate form of poly(lactic-co-glycolic) acid (abbreviated as PLGA) [16]

etc. are used. All of these modern polymers are used as prefabricated scaffolds to fill bone defects [9]. However, the polymers have low Young's modulus and low creep resistance compared to bone [10]. This limits their usage on biomedical applications and clinical surgery.

In addition to these polymers, polymer matrix composites (PMCs) reinforced with ceramic particles (i.e., HAp, bioglass) [15] and carbon fibres [11] are used. The focus on PMC is important to develop mechanical properties as well as the bioactivity and biointegration. It is well known that bone is a composite of organic (collagen) – inorganic (calcium phosphate) phases and the replacement material should be a similar composite. Porous biodegradable PMCs reinforced with HAp particles with suitable organic to inorganic ratio should fit and integrate with the bone better conserving the mechanical properties of the bone [10].

1.2.2.6. Porous HAp

HAp has found a significant place to be used as synthetic bone grafting applications to fill bone defects. HAp has a similar composition and structure with the natural bone, and this allowed it to be used in a wide-range of applications. Generally HAp powders are produced by solid state, wet chemical and hydrothermal methods [17, 18] and then sintered at between 700 °C and 1300 °C to obtain bulk crystalline forms [8]. Although, the HAp itself is highly

biocompatible, osteointegrative, and osteoconductive; the dense and highly crystalline HAp ceramics have low absorption rate in the physiological environment due to its chemical stability [8, 19]. As a result, porous HAp scaffolds are produced in order to increase integration ability and dissolution rate.

The first attempt to produce porous HAp scaffolds goes back to 1970's. During these years, a process to convert corals (having a similar composition with nacres) into a porous network of HAp was utilized in Pennsylvania State University [20]. The calcium carbonate in the coral was reacted with diammonium hydrogen phosphate ($(NH_4)_2HPO_4$) and converted hydrothermally (taking advantage of the low temperature and high pressure) into pure HAp. The product was the exact replica of the coral skeleton including the interconnected porosity [21] which is also similar to the bone structure of the human body [8].

In those years, a synthetic alternative of the coral-converted HAp was produced and named as Coralline™ HAp and marketed as Pro Osteon™. The aim for production of Coralline™ HAp is to create an implant with interconnected pore network with regular pore size mimicking the porous structure of the coral-converted natural HAp. The production method consists of adding hydrogen peroxide in the synthetic HAp, prior to compaction and heat treatment. During heat treatment, hydrogen peroxide will create bubbles leaving a porous network after cooling. The porous structure has low mechanical properties, however; its interconnected porous structure allows fast bone ingrowth into the implant. This increases osteointegration and biocompatibility of the Coralline™ HAp compared to coral-converted HAp.

Porous HAp ceramics can also be produced with polymers or natural polymeric materials, i.e. sponges. The porous structure is obtained by mixing the polymer component with HAp slurry and burning the polymeric phase. This operation leaves a porous network of HAp. By this method, the porosity can be increased up to 75% - 95% which is similar to the cancellous bone [22, 23].

Figure 1.5 An optical image of Pro Osteon™ [16]

Another technique for production of porous HAp scaffolds is ceramic foaming method. Foaming agents like hydrogen peroxide, carbonate salt or baking powder are added to the HAp slurry. The foaming agents go into gas evaporating reactions and the gas creates a porous HAp network. The resultant HAp was sintered at the end of the procedure. Additionally, using this technique, gel casting of HAp is possible. Gel casting involves a crosslinking polymerization step that gelatinizes the foam-like HAp slurry rapidly to form an interconnected porous structure [22].

A novel approach to produce porous HAp is converting gypsum ($CaSO_4 \cdot 2H_2O$) to HAp by hydrothermal methods. Gypsum is used as mold for slip or pressure casting in ceramic industry and it has high porosity. These gypsum molds becomes old after repeated usage and discarded. It is possible to recycle them as a filter system for purifying water after converting to HAp using diammonium hydrogen phosphate up to 15 days of reaction times [24] and therefore, lead ions dissolved in DI-water were successfully removed by the HAp produced by this method [25]. The reaction time can be as short as 2 min if microwave-hydrothermal methods

were used [26].More recently, producing bulk plaster of paris (PoP) or gypsum freeform structures by 3D printing method and converting them to HAp by wet chemistry methods was studied. The HAp was produced by immersing PoP and gypsum bulk structures to diammonium hydrogen phosphate solution at 80 °C and reacted for 2 to 24 h [27, 28]. Moreover, after heat treatment of the converted bulk structures at 1150 °C, β-tricalcium phosphate was obtained [27].

1.2.2.7. Ceramic cements

The ceramic cements, such as glass ionomers, calcium sulfate and calcium phosphate-based ceramics has an important role in biomedical applications. The setting property of the cements can be used in to fill irregular defects of the bone. Good biocompatibility, osteoconduction and excellent absorption properties utilized cements to be safely used in the physiological environment.

The first documented bone repairing operation goes back to 10^{th} century. The Arabs used calcium sulfate (as plaster of paris, PoP, $CaSO_4 \cdot 0.5H_2O$ and its hydrated from gypsum $CaSO_4 \cdot 2H_2O$) to fix the broken limb externally. In 19^{th} century, a Dutch army surgeon combined PoP into bandagable form, which is similar to today's practice to fix bone fracture externally. The first surgical successful implantation was done by Dreesmann to treat bone tuberculosis [8]. In 20^{th} century, more comprehensive study on calcium sulfate cements was done by Peltier et. al., and they concluded that due to its good osteoconductive and osteointegrative properties, calcium sulfate can be used for internal surgery to fill bone defects, however; it should be implanted adjacent to the periosteum tissue [29]. The absorption rate of calcium sulfate in physiological environment is 5 to 7 weeks. Although, the mechanical properties of calcium sulfate cements are low [8], the calcium sulfate is gaining attention in today's clinical practice [30], however; the application areas of calcium sulfate cements are still limited [31]. Additionally, the setting reaction is exothermic and the released heat damages the tissues surrounding the implant.

A different kind of cement was also introduced for dental use, called glass ionomers. This cement is composed of calcium/aluminum/fluorosilicate glass

powder mixed with polycarboxylic acid. The components react with each other by an exothermic reaction with CO_2 gas evolution. The gas evolution creates a porous structure. The chemical and physical structure creates osteoconductive and osteointegrative conditions within the implant and the surrounding tissues. This cement is water-insoluble and therefore; cannot be used as bone replacement. However; glass ionomers obtained an important role in dental industry to replace PMMA cements [8].

A wide range of calcium phosphate cements were utilized as bone cements. The important ones are alpha-tricalcium phosphate (α-$Ca_3(PO_4)_2$, abbreviated as α-TCP) and beta-tricalcium phosphate (β-$Ca_3(PO_4)_2$, abbreviated as β-TCP). They are easily absorbed and integrated by the living body up to 18 months after implantation. They are usually marketed as mixtures of monocalcium phosphate monohydrate ($Ca(H_2PO_4)_2 \cdot H_2O$), tetracalcium phosphate ($Ca_4(PO_4)_2O$), dicalcium phosphate ($CaHPO_4 \cdot 2H_2O$), octacalcium phosphate ($Ca_4H_2(PO_4)_6 \cdot 5H_2O$), calcium deficient ($Ca_9(HPO_4)(PO_4)_5OH$) and stoichiometric HAp to increase their chemical properties [1, 4, 8, 11]. These mixtures or TCP alone transforms into a set porous body at physiological temperatures by cement type hydration. Moreover, their setting time is as low as a few minutes in addition to low heat generation during setting reaction. [1, 8]. In addition to these advantages, they do not need to be delivered in prefabricated forms, although they can be. The main idea of delivering them in powder form is their injectibility in cement form [4]. In bulk form, they can be used as pre-shaped porous bone fillers and they would be better than solid HAp blocks [1].

The main advantages of the calcium phosphate cements are their high biocompatibility, high bioactivity, good osteoconduction and osteointegration properties. However; they have poor mechanical properties and they can only be used in non-load bearing applications, such as drug delivery systems [1].

To summarize, scaffold materials used as bone replacements in biomedical applications should have following properties:

- The material should be biocompatible.
- The material should be biodegradable.
- The material should degrade in the same rate as the living body repairs the tissue.
- During degradation, the material should not produce toxic components.
- The scaffolds should be highly porous with interconnected porosity that allow tissue ingrowth
- The mechanical properties should match with the real bone.

It is possible to obtain all of these properties in ceramic implants after certain modifications, such as coating or mixing with polymeric materials.

1.2.3. Improving the mechanical properties of bone substitutes

In biomedical industry, the ceramic materials for implants are the most common choices. As previously considered, ceramic materials have poor mechanical strength and in order to use them as implants, their strength should be increased but implants should not lose their biocompatibility. Most common way to increase mechanical properties of ceramic materials is combining them with biodegradable polymers which are completely absorbed by the living body when implanted. Biodegradable polymers are successfully used in clinical surgery and they have no known inflammatory issues in the living body.

The biodegradable polymers are, in general, natural materials; such as silk, collagen, starch, chitin, chitosan, hyaluronic acid, fibrin, alginates and some others are synthetic materials; such as polylactic acid, polyglycolic acid, polycaprolactone, poly-hydroxybutyrate etc. The synthetic materials have gained popularity in biomedical applications and clinical surgery as well as the natural materials. Although, there are compromising studies on all biodegradable polymers discussed in some review papers [9-11], this thesis was focused on applications of polycaprolactone (PCL) polymer.

PCL is a biodegradable polymer, synthesized by ring opening reaction of ε-caprolactone. It is sometimes called as poly(ε-caprolactone). Its melting point is 60 °C. PCL, alone, is generally used for drug delivery and dental applications. Its nylon-like behavior allows PCL to be used for rapid prototyping applications [32]. Additionally, it releases non-toxic monomers upon degradation in physiological environment [9, 11].

PCL/HAp composites combine biocompatibility and bioactivity by forming a function surface between the living tissues with acceptable mechanical properties, increase in compression and tensile strength as well as the resilience [10]. Previously it was found that, PCL/HAp composites produced by solvent casting increases mechanical properties compared to uncoated samples [33]. The PCL to HAp ratio in PCL/HAp composites also plays an important role in their mechanical properties. Using an appropriate PCL to HAp ratio, the compression strength can be increased up to 5 times [23]. This is a common practice when the ceramic scaffold is coated with polymers [15, 34].

Table 1.1 Mechanical properties of the bone and some implants [8]

Type of implant / bone	Compressive Strength (MPa)	Tensile Strength (MPa)
Cancellous bone	5.5	3
Cortical bone	162	151
Gypsum	23	4.1
Porous HAp	60	2.5
PMMA	90	6.9
Porous alumina	60	15
Bioglass	-	42
A/W glass-ceramic	-	215
Bioglass (PS modified)	-	103
Glass ionomer	180	-

1.3. Objective and structure of the thesis

The main objective of this study was to produce hydroxyapatite (HAp) powders from commercial grade impure plaster of paris ($CaSO_4 \cdot 0.5H_2O$, PoP) under ambient (at 1 atm, 25 °C, 50 °C and 90 °C) and hydrothermal-like (120 °C and 2 ± 0.2 atm) conditions using di-ammonium hydrogen phosphate ($(NH_4)_2HPO_4$) solution. This objective was later expanded to produce HAp in powder and bulk form gypsum ($CaSO_4 \cdot 2H_2O$) under hydrothermal-like conditions. Moreover, the chemical, physical and morphological analyses were performed on the products. Additional objectives were investigation of chemical and physical properties of HAp after heat treatment and the comparison of the mechanical properties of polycaprolactone (PCL) coated bulk HAp samples with uncoated bulk HAp samples. These objectives were achieved and presented in three parts in the thesis.

In the first part, morphology, chemical and physical properties of commercial grade PoP powders and the hydration products thereof, i.e. gypsum were investigated. These studies included chemical and phase analyses, particle size determination and morphological examinations, and porosity measurements for the hydrated bulk gypsum formed with different solid to liquid ratio.

The second part is the synthesis and conversion of HAp from commercial grade impure PoP under ambient conditions using 1 M of $(NH_4)_2HPO_4$ solution. This conversion reaction was also examined under hydrothermal-like conditions using PoP with 0.5 M and 1 M of $(NH_4)_2HPO_4$ solutions. Additionally, the conversion reaction under hydrothermal-like conditions was further expanded to form HAp using gypsum as a precursor. The effect of pressure, solution chemistry and time on the conversion reaction was investigated. Phase and morphological analyses was performed on all samples. Furthermore, porosity measurements of the converted HAp pellets were performed.

In the final part, the exact chemical identity and the mechanical properties of the products were examined. Exact chemical identity of the products was investigated by heat treating the chosen samples up to 1200 °C for 2 hours. After heat treatment

process, phase analyses were performed on the heat-treated samples. For mechanical investigations, HAp pellets converted from gypsum pellets under hydrothermal-like conditions were used. The effect of porosity and the PCL coating on fracture strength of the bulk HAp pellets were investigated by using diametrical compression test.

CHAPTER 2

MATERIALS AND METHODS

2.1. Materials

Commercial grade partially hydrous form of calcium sulfate ($CaSO_4 \cdot 0.15H_2O$, plaster of paris or PoP powders, Knauf™) is used as a starting material to synthesize HAp powders and HAp bulk forms. This was the major precursor material for this thesis. The physical properties and chemical analysis of PoP powders will be introduced in the following Results chapter. Di-ammonium hydrogen phosphate ($(NH_4)_2HPO_4$, 99.0% pure) is obtained from Merck (catalog no. 1.01207.0500). Ethanol (or EtOH C_2H_5OH, 99.8% pure) is obtained from Riedel-de Haen (catalog no. 32221).

The hydrothermal reaction vessel used in conducting hydrothermal reactions is a pressure cooker shown in Figure 2.1. The vessel was modified to handle more water inside. Additionally, to make the sample container stationary and to avoid spilling of the reactants into the vessel a simple fixation setup was used.

Besides pure HAp pellets, composites were also produced in the final stages of the work. The polymers in the form of thin films were coated on bulk HAp forms. A biodegradable polymer – polycaprolactone ($C_6H_{10}O_2$, PCL, $M_n \approx 80000$, 99% pure) which was obtained from Aldrich (catalog no. 440744) was used. The solvent was chloroform ($CHCl_3$, 99.8% pure) which was obtained from Sigma-Aldrich (catalog no. 34854).

Figure 2.1 A view of pressure vessel used in high pressure experiments. (left: general view, right: interior part showing the modification). This modification was done to put more water inside. Additionally, it has made the sample container stationary and disabled the opportunity of sample spilling into the vessel.

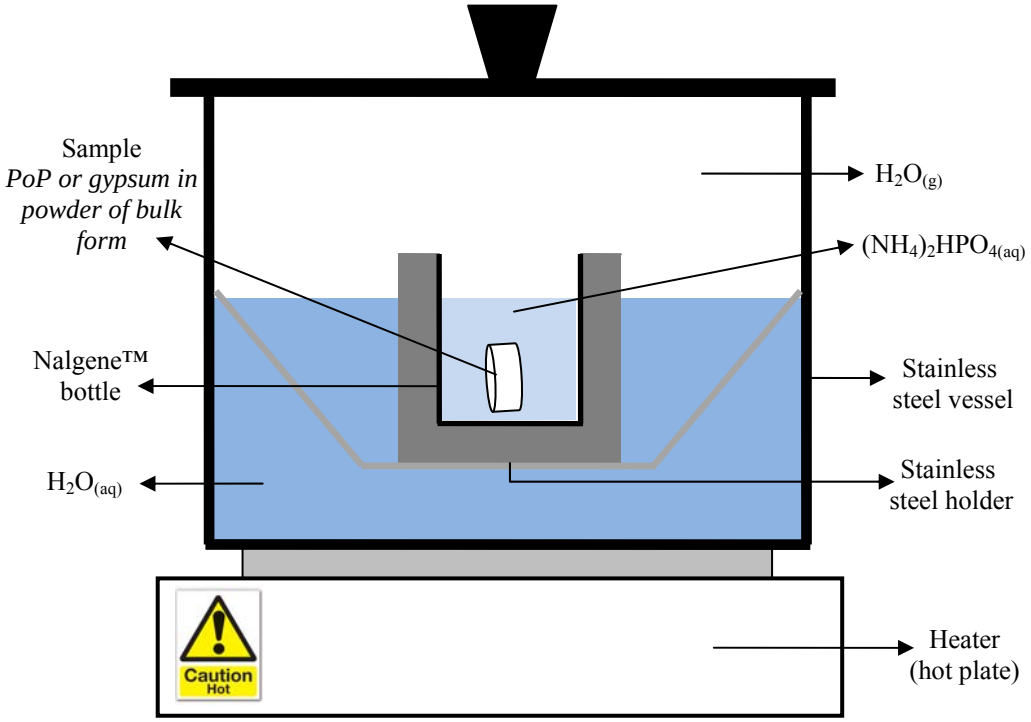

Figure 2.2 Schematic representation of the experimental setup for hydrothermal-like conversion studies of calcium sulfate to HAp

2.2. Experimental procedures

2.2.1. Setting (hydration) of PoP

A hardened form of calcium sulfate, gypsum (calcium sulfate dihydrate, $CaSO_4 \cdot 2H_2O$) can be produced by mixing partially hydrous forms of calcium sulfate powders with water. According to *Reaction 2.1*, 4 g of PoP was mixed with 2.4 mL DI-water to obtain gypsum.

$$(CaSO_4)_2 \cdot H_2O + 3H_2O \longrightarrow 2(CaSO_4 \cdot 2H_2O) + \text{Heat} \qquad \textbf{(2.1)}$$

The reaction may not be fully effective in converting all reactants into gypsum but some PoP may remain as unreacted in the products. The conversion reaction is exothermic. In the preliminary studies, the gypsum products obtained by this way analyzed using x-ray diffraction (XRD) and scanning electron microscopy (SEM) analyses to reveal the typical morphological and chemical changes upon hydration (setting) of PoP.

2.2.2. Conversion of calcium sulfates into hydroxyapatite (HAp)

2.2.2.1. Synthesis of HAp powders from PoP powders

HAp synthesis from PoP powders was achieved by two routes. The flowchart in Figure 2.3 shows the details for conversion of PoP powders to HAp. In Route-1, HAp was synthesized in powder form under *ambient* conditions using different temperatures to verify the effect of temperature on reaction kinetics. This conversion was achieved according to *Reaction 2.2*.

$$10CaSO_4 \cdot 0.15H_2O + 6(NH_4)_2HPO_4 \longrightarrow Ca_{10}(PO_4)_6(OH)_2 + 6(NH_4)_2SO_4 + 4H_2SO_4 + 1.4H_2O \qquad \textbf{(2.2)}$$

In this route, a water bath was used to achieve constant reaction temperature. First, 5.3 g of $(NH_4)_2HPO_4$ was added into 40 mL of DI-water in order to produce 1 M of $(NH_4)_2HPO_4$ solution. This was achieved through continuous stirring with the help of a magnetic bar on a hot plate for 5-10 min. Then, 4 g of PoP was mixed with the 40 mL solution in a plastic container floated in the water bath. The temperature of

the water bath was set 25 °C, 50 °C and 90 °C. The reaction time changed from 2 to 6 hours.

In Route-2, HAp was produced using a *hydrothermal vessel* to see the effect of pressure on the conversion kinetics of PoP powders to HAp. To achieve this goal, first, predefined amounts of $(NH_4)_2HPO_4$ was dissolved in DI-water to form 1 M or 0.5 M solutions of $(NH_4)_2HPO_4$, by dissolving 5.3 g or 2.6 g of $(NH_4)_2HPO_4$ in 40 mL of DI-water through continuous stirring on a hot plate for 5-10 min. Then, PoP powders (4 g) mixed with 40 mL of $(NH_4)_2HPO_4$ solution in 100 mL high density polyethylene (HDPE) Nalgene™ bottle. The bottle was cut from its neck to increase the pressure-affected area. After cutting operation, the volume of the bottle was reduced to 80 ml. After mixing the solution and the precursor in the HDPE Nalgene™ bottle, the bottle was put inside the pressure vessel shown in Figure 2.1. The remaining space of the pressure vessel was filled with approximately 5 lt of boiled DI-water and the top cover of the pressure vessel was closed. Then, the pressure vessel was placed on a hot plate set to 200 °C. The pressure value was 2 ± 0.2 atm inside the chamber. The pressure value data was obtained from the producer. As a result, the temperature inside the chamber was calculated from pressure-temperature equilibrium phase diagram of H_2O as 120 °C. These conditions, i.e. approximately 2 atm and 120 °C, will be referred as standard hydrothermal-like conditions throughout the thesis. The reaction time varied from 15 min to 12 h.

At the end of the reaction period, the solid products are taken out of the plastic container in both processing routes. The products were washed with DI-water and filtered to eliminate any salt remains, such as ammonium sulfate ($(NH_4)_2SO_4$), hydrogen sulfate (H_2SO_4) or any other residues. After filtering operation the residue was put in open air drying oven operating at 75 °C for 1 day. Figure 2.4 summarizes the experimental design and the process parameters examined for this conversion process.

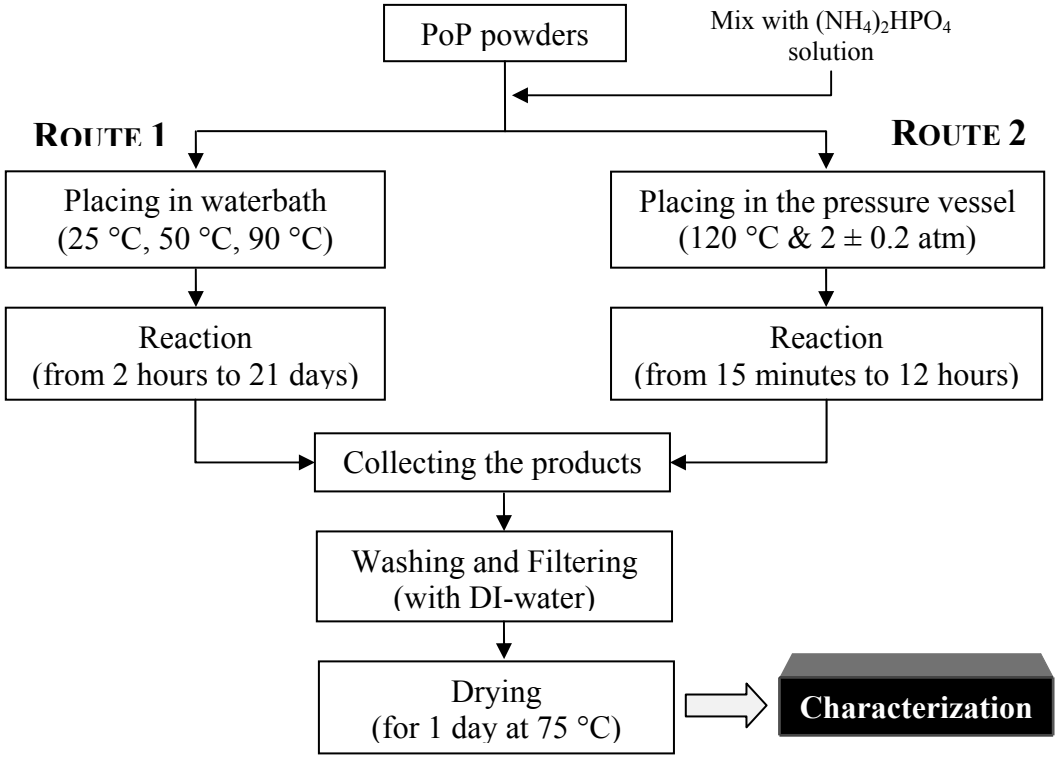

Figure 2.3 Experimental procedure for synthesis of HAp from PoP powders

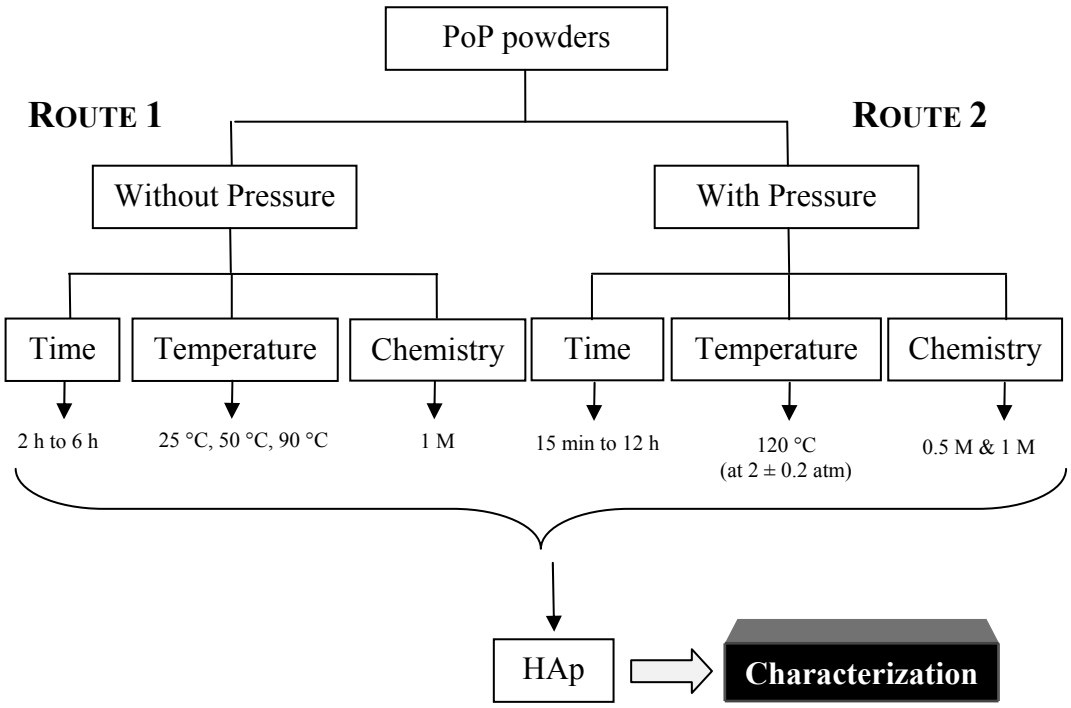

Figure 2.4 Experimental design of HAp synthesis from PoP powders

2.2.2.2. Synthesis of HAp powders from gypsum powders

In the second part of the experimental work, gypsum powders were first formed by full hydration of PoP powders. Then, attempts for converting the gypsum product into HAp have been performed. First, PoP powders were reacted to form gypsum according to *Reaction 2.1*. To obtain gypsum powders using this reaction, 4 g of PoP powder were mixed with 2.4 mL of DI-water with a solid to liquid (*s:l*) ratio of 1.67 and this mixture was dried for 1 day at 25 °C. After the drying, a bulk hardened sample of set gypsum was obtained. This bulk sample was grounded using agate mortar and pestle to powdered gypsum. HAp conversion of the gypsum powders was achieved according to below given *Reaction 2.3* and at standard hydrothermal-like conditions (120 °C, 2 ± 0.2 atm) as explained in the previous section.

$$10CaSO_4{\cdot}2H_2O + 6(NH_4)_2HPO_4 \longrightarrow Ca_{10}(PO_4)_6(OH)_2 + 6(NH_4)_2SO_4 + 4H_2SO_4 + 18H_2O \quad \textbf{(2.3)}$$

The flowchart in Figure 2.5 shows the details for conversion of gypsum powders to HAp and Figure 2.6 summarizes the experimental design and the process parameters examined for this conversion process.

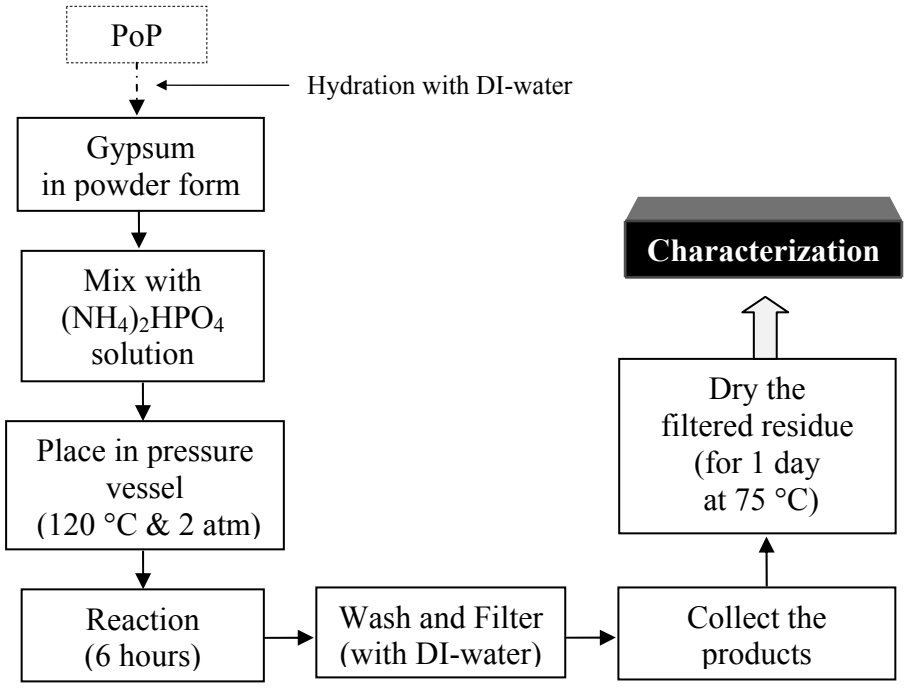

Figure 2.5 Experimental procedure for synthesis of HAp from gypsum powders

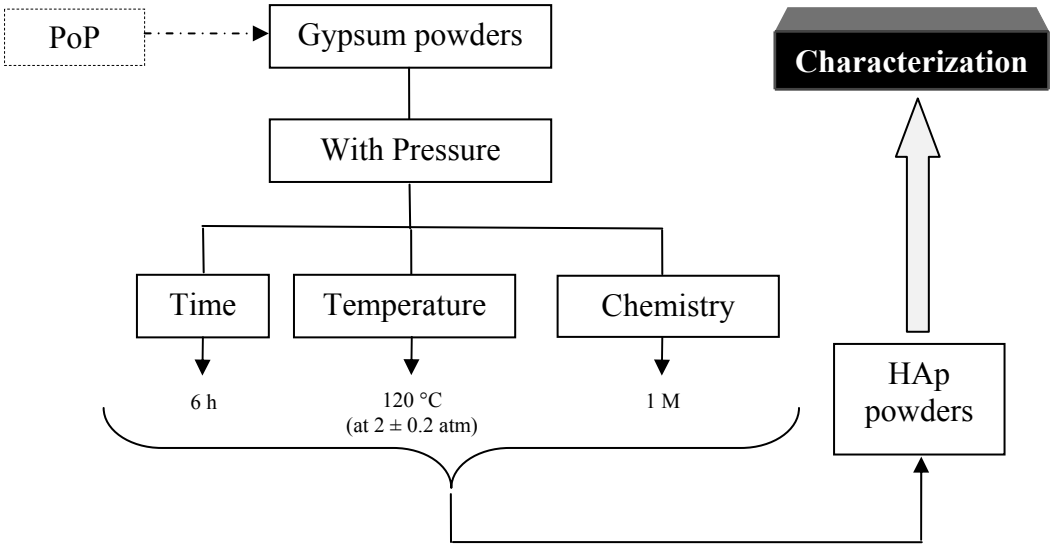

Figure 2.6 Experimental design of HAp synthesis from gypsum powders

2.2.3. Hydrothermal-like synthesis of bulk HAp

2.2.3.1. Processing of bulk gypsum pellets

In order to synthesize HAp in bulk form, first, gypsum pellets were prepared according to *Reaction 2.1*. These pellets simply served as pre-form, which were converted to HAp afterwards. To produce disc-shaped preforms, a polyethylene mold with 45 openings was used, shown in Figure 2.7. The diameter and the height of the openings are 15 mm and 6 mm, respectively. Simply partially wet slurry of PoP-DI-water was packed into the disc-shaped openings and in situ setting of the mixture to gypsum was allowed. After setting the pellets dried for 1 day at 25 °C and then they were taken out from the mold.

The gypsum pre-forms were produced to achieve different porosities in the structure. In order modify the porosity different *s:l* ratios were employed. The gypsum pellets were produced using *s:l* ratios of 1.33, 1.67, 2.22, 3.33. The amount of solid (PoP) and liquid (DI-water) used for producing bulk gypsum samples are shown in Table 2.1.

2.2.3.2. Synthesis of bulk HAp from gypsum pellets

The dried bulk gypsum samples then, converted into HAp using the previously explained standard hydrothermal-like conditions (120 °C, 2 ± 0.2 atm) upon reacting with 1 M $(NH_4)_2HPO_4$ solution.

The flowchart in Figure 2.8 shows the details for conversion of gypsum powders to HAp and Figure 2.9 summarizes the experimental design of this conversion process.

Table 2.1 The amount of PoP powder and H_2O used to produce bulk gypsum samples for different solid to liquid (*s:l*) ratios.

Amount of PoP powder (g)	**Amount of H_2O (g)**	**Solid to liquid (*s:l*) ratio**
1.23	0.92	1.33
1.33	0.80	1.67
1.41	0.64	2.22
1.92	0.58	3.33

Figure 2.7 The mold used to produce disc shaped bulk gypsum samples

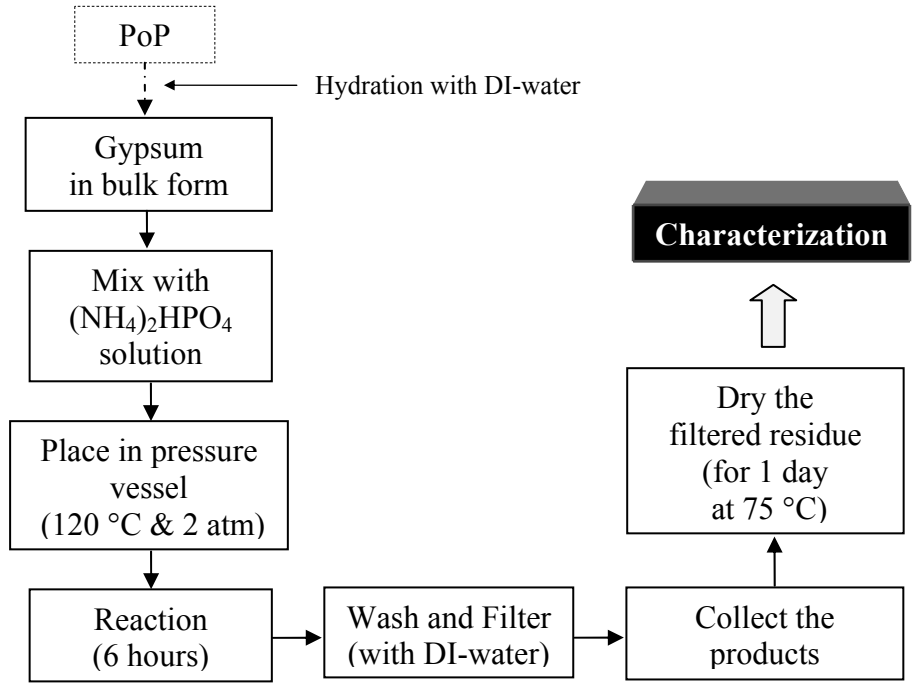

Figure 2.8 Experimental procedure for synthesis of bulk HAp from gypsum pellets

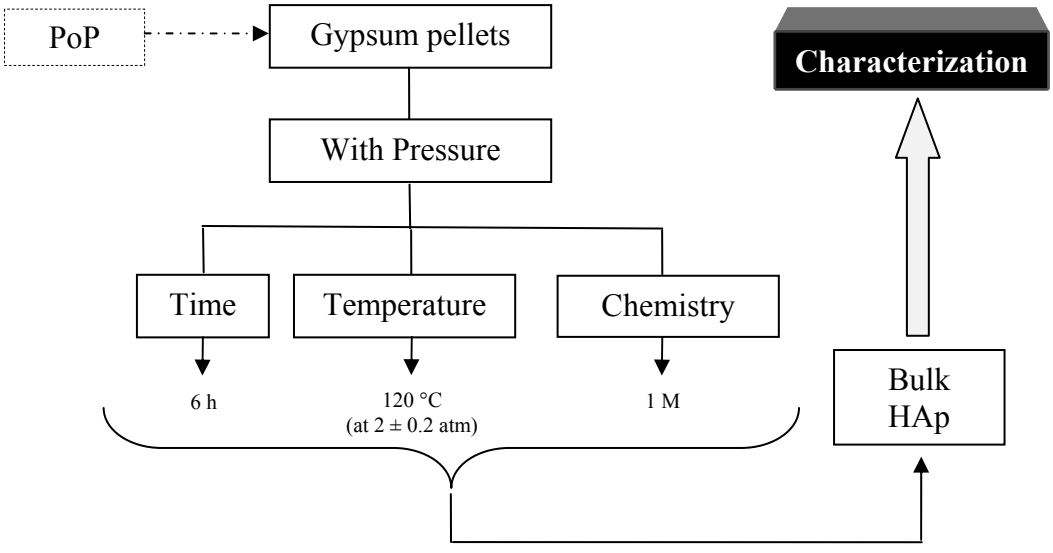

Figure 2.9 Experimental design of HAp synthesis from gypsum pellets

2.3. Material Characterization

2.3.1. X-ray diffraction (XRD) analysis

XRD measurements were employed for the phase analysis of PoP powders, gypsum reactants as well HAp products. The analyses were performed by Rigaku X-Ray Diffractometer (Ultima D/MAX2200/PC). CuKα radiation was used as an X-ray source at 40 kV. The scan speed was 2°/min. The samples were scanned over from 20º to 40º in 2θ.

2.3.2. Scanning electron microscopy (SEM) analysis

Morphology of the samples was studied by SEM. SEM analyses were performed by using a Jeol JSM-6400 Electron Microscope, equipped with a NORAN System 6 X-ray Microanalysis System and Semafore Digitizer. Powders and bulk samples were coated by Au-Pd alloy by an Anatech HUMMLE VII sputter coating device.

2.3.3. Particle size analysis

Initial particle size analysis of PoP powders was investigated. Particle size analysis was performed by using Malvern Mastersizer 2000 particle size analyzer device using dry method.

2.3.4. X-Ray fluorescence (XRF) analysis

The chemical analysis of the starting commercially available PoP powders was achieved by XRF. The qualitative and quantative analyses were performed by BRUKER S8 Tiger XRF device by elemental analysis method. The device was operated with 60 KV tube voltage, Rh target material and Cu filter and additionally, all experiments were performed under ambient (He gas) conditions. Scanned spectrum size was between 0.5 and 50 KeV.

2.3.5. Density and porosity measurements

The porosity of the gypsum and HAp pellets were determined by density measurements. The bulk density was determined using xylene penetration technique (Archimedes's method). The samples were weighed in their dry (m_{dry}),

saturated (m_{sat}) and suspended (m_{sus}) form. The density measurement was done according to the *Equation 2.1*.

$$Density = 0.86 \times \frac{m_{dry}}{m_{sat} - m_{sus}} \qquad \textit{(Eqn 2.1)}$$

To find porosity, obtained experimental density values were divided into theoretical density of the gypsum which is 2.308 g/cm^3 and HAp which is 3.156 g/cm^3.

2.3.6. Processing and characterization of polymer-coated HAp composite pellets

The HAp pellets converted by hydrothermal-like conditions from gypsums pellets were coated with polycaprolactone (PCL). The coating was performed by immersing HAp pellets into dilute PCL solution. HAp pellets obtained from only one set gypsum performs (with a *s:l* ratio of 1.33 corresponding to a certain porosity) were coated with polymer. The main objective was to examine the change in mechanical properties compared to their counterparts, i.e pure HAp pellets of identical microstructural properties. Typically, coating was achieved by dipping HAp pellet into 5 wt% PCL-chloroform solution. The coating operation was repeated subsequently 5 times to ensure deposition of adequate material in a thin film coating form. The trials with more concentrated polymer solutions were not successful, as PCL-chloroform solution took a gel-like thick form at higher loadings. After each coating operation, the samples were dried for 1 hour at 25 °C before applying the following immersion step.

Finally, examinations were performed to evaluate the efficiency of the polymer coating process, and to ensure presence of coating on HAp pellets. This is achieved by heating polymer-coated HAp composite pellets to 200 °C in open air furnace, to eliminate the polymer coating by burning. The weight change of the pre- and post-heat treated samples was measured in order to evaluate the feasibility

of the coating study. Additionally, the microstructure of polymer coated pellets was examined by SEM studies.

2.3.7. Measurement of mechanical properties

The fracture strengths of HAp pellets and polymer-coated HAp structures were determined using diametrical compression test [35]. Schematic representation of the diametrical compression test is shown in Figure 2.10. The tests were performed using Shimadzu AGS-J 10 kN universal testing machine with cross-head speed of 0.5 mm/min at 25 °C.

The maximum tensile strength (or fracture strength), which occurs on the diametrical plane between loading points, is given in *Equation 2.2* [36, 37].

$$\sigma_f = \frac{2P}{\pi D t} \qquad \textit{(Eqn 2.2)}$$

Where P is the load applied on the diametral axis, D is the sample diameter and t is the sample thickness. The flats on the Shimadzu universal testing machine were covered with a padding material (i.e. paper towel) in order to distribute the applied load homogeneously and compensate the effect of irregularities on the specimen surface. Typically 8-10 pellets were broken to obtain statistically relevant and representative strength values for each class of samples.

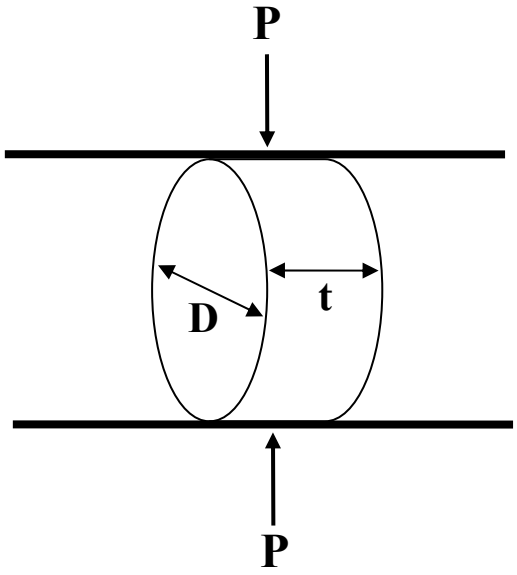

Figure 2.10 Schematic representation of diametrical compression test. In the figure, *D* is the diameter of the pellet, *t* is the thickness of the pellet, *P* is the load applied diametrically on the pellet.

CHAPTER 3

RESULTS AND DISCUSSION – I

Characterization of starting materials and preliminary evaluations of PoP to gypsum conversion

This section includes the characterization results for the commercial grade PoP powders used as the major starting material in this study. The initial step of this characterization is chemical analysis of the PoP powders. Since commercial grade PoP powders were used throughout the experiments, the chemical analysis of the starting PoP powders is a crucial step to further investigate its conversion to gypsum via hydration. The chemical analysis was done using XRF. In addition, phase characterization was performed by XRD.

The second step is the determination of the physical properties for PoP powders. This includes particle size analyses by laser diffraction techniques in combination with SEM examinations. The purpose of these analyses was to complete the characterization of the commercial grade PoP powders.

In some studies, PoP was hydrated to form gypsum before converting gypsum to HAp. This hydration reaction will be also referred as *setting reaction* throughout the thesis. The physical and chemical changes achieved by the setting reaction were also determined in this part of the thesis using mainly XRD analyses.

The final step of this chapter is the analyses of the physical and chemical aspects of the hydrated form of the PoP powder, i.e. the properties gypsum the bulk

hardened product of the setting reaction. Bulk gypsum pellets were produced using different solid to liquid (PoP:H_2O, abbreviated as *s:l*) ratios and related porosity change was also determined. XRD and SEM analyses were performed on these bulk forms of gypsum pellets.

3.1. Characterization of PoP powders

The chemical analysis results for PoP powder are shown in Table 3.1. The examination showed that starting PoP powders includes strontium, a volcanic glass called perlite (an alumina-silicate glass with elemental silicon) and other impurities. Strontium is known present as strontium sulfate with natural deposits of calcium sulfate ore [38, 39].Perlite is usually added to PoP intentionally to increase the permeability of the PoP and gypsum. This point will be further discussed together with the SEM examination in the upcoming sections.

The particle size analysis results (obtained by laser diffraction method) in Figure 3.1 shows that the average particle size of the PoP powders was 54.7 ± 3 μm. No pre-treatment was applied to the powders before particle size analysis. According to Figure 3.1, the particle distribution seems to be divided into three major size groups. The vast amount of the powders has an approximate particle size of 7 μm, another variety of the powders have an approximate particle size of 65 μm and the remaining variety has an approximate average particle size of 500 μm.

The SEM analysis of the PoP powders in Figure 3.2 reveals the average particle size and the initial morphology of the PoP powders. The average particle size of PoP powders is about 50 μm comparable with the data of measurements performed by laser diffraction methods. The morphology of the PoP powders is prismatic and equiaxed in shape, which is a typical appearance for the α-polymorph of calcium sulfate.

Table 3.1 The chemical analysis (obtained using XRF by normalizing the values to 100%) of the starting PoP powders (ppm level elements are ignored)

Elements	Ca	S	Sr	Si	Mg	Fe	Al
Amount (in wt%)	63.6	32.4	2.63	0.56	0.28	0.18	0.13

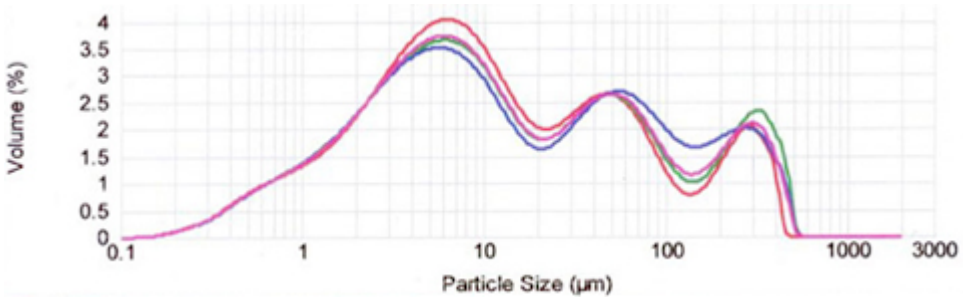

Figure 3.1 Particle size distribution of PoP powders obtained using laser diffraction methods (average particle size: 54.7 ± 3 µm)

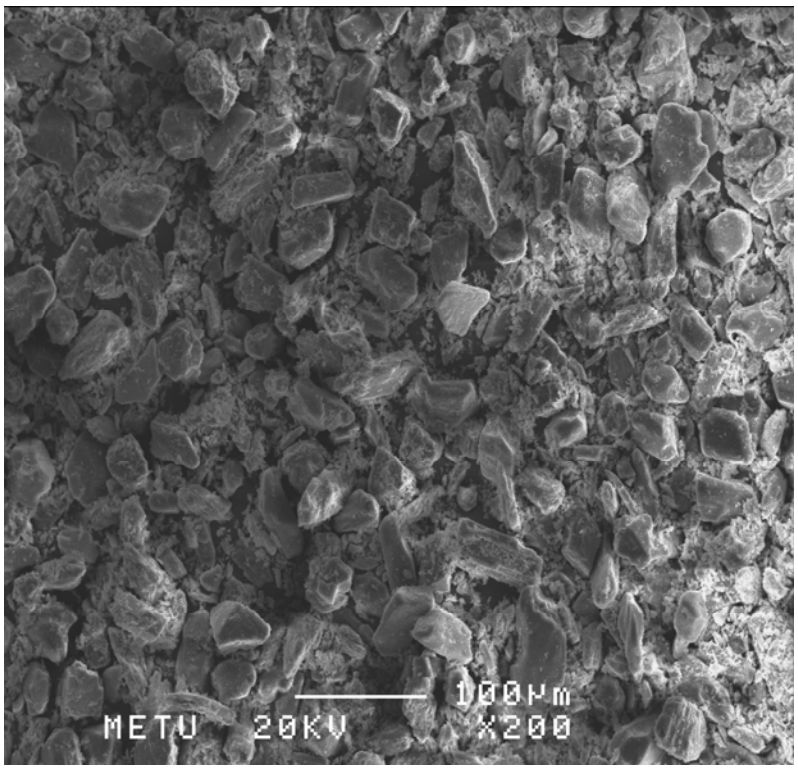

Figure 3.2 SEM micrograph of PoP powder. The morphology of the powders is prismatic and equiaxed with an average size around 50 µm. This typical appearance shows that the starting PoP powders are in α-polymorph of calcium sulfate hemihyrate.

The XRD diffractogram of PoP powders is shown in Figure 3.3. The pattern matches with that of JCPDS card no. 23-128 for $CaSO_4 \cdot 0.15H_2O$. Additionally, as illustrated in Figure 3.3, PoP contains same impurity phase (labeled as *Unidentified Phase 1*) has an unidentified phase which does not match with any standard JCPDS card.

3.2. Characterization of PoP hydration product: Gypsum

The PoP powders were hydrated with DI-water using an *s:l* ratio of 1.67 to form gypsum at 25 °C. The gypsum samples were dried for 1 day at 25 °C and grounded to powder form. The XRD diffractogram of the gypsum powders shown in Figure 3.4, illustrates that a complete transformation of PoP to did not proceed. A small amount of PoP remains unreacted after the setting reaction. The set powders' XRD pattern matches with JCPDS card no. 33-311 for $CaSO_4 \cdot 2H_2O$, i.e. gypsum. Additionally, the initial unidentified phase, shown in Figure 3.3**,** converts into some other phase (labeled as *Unidentified Phase 2*) after hydration that still does not match with any known JCPDS card.

Additionally, phase analysis of the hydrated bulk samples obtained by hydration of preformed PoP pellets was performed for *s:l* ratio of 1.67. The results are shown in Figure 3.5. In the bulk samples, again, complete transformation to gypsum is not observed similar to the powder samples. The gypsum product is indentified again with JCPDS card no. 33-311, the remaining phase matches with JCPDS card no. 23-0128.

SEM micrographs of the hydrated bulk samples are shown in Figure 3.6. It was found that a typical hydrated bulk sample has three different microstructure regions labeled in Figure 3.6. These are set and hardened needle-like gypsum regions (labeled as region 1), perlite region (labeled as region 2) and porosities(labeled as region 3). The microstructure shown in Figure 3.6b (representative for region labeled as 1) is produced by transformation of prismatic-

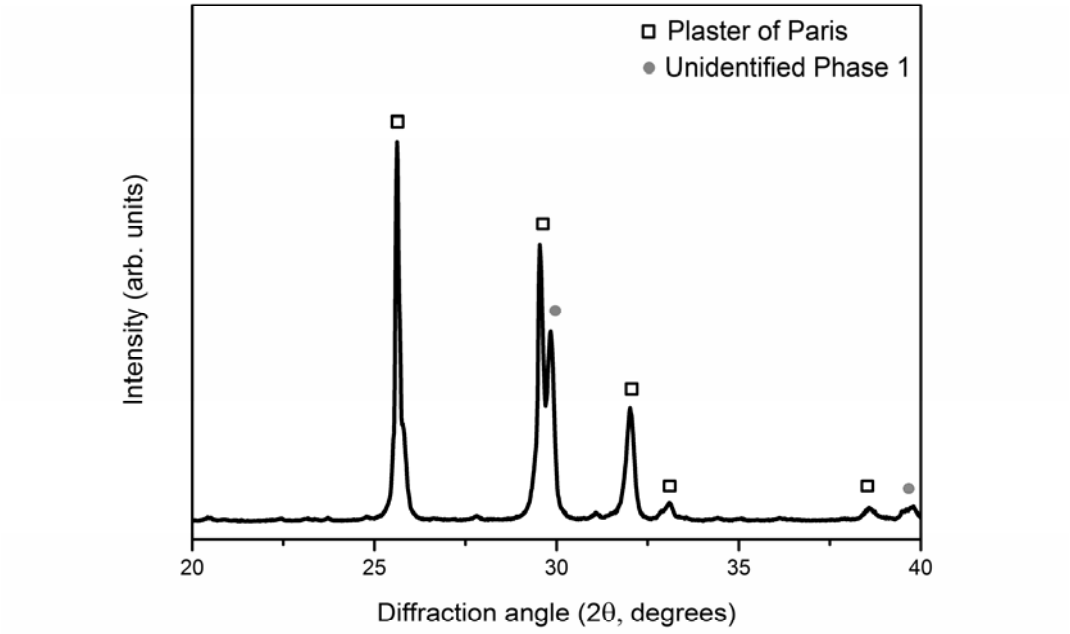

Figure 3.3 XRD diffractogram of PoP powder.

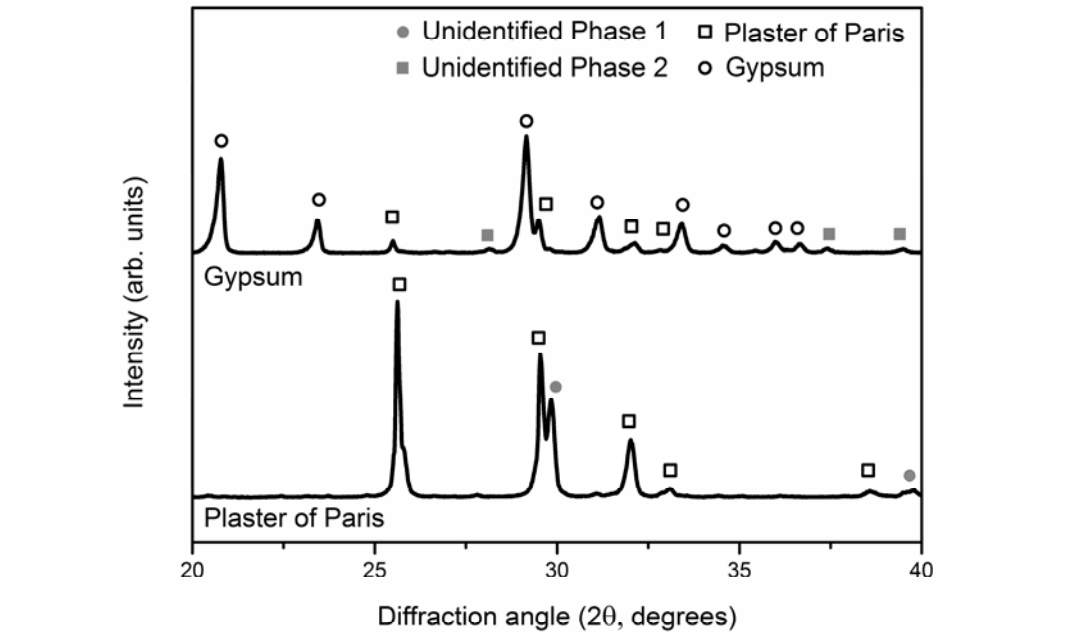

Figure 3.4 A comparison of the XRD diffractograms PoP powder and gypsum after setting with H_2O, drying at 25 °C for 1 day and grinding to powder form. As shown in the diffractograms, some PoP remains in the gypsum structure and complete conversion from PoP to gypsum is not achieved through the hydration reaction.

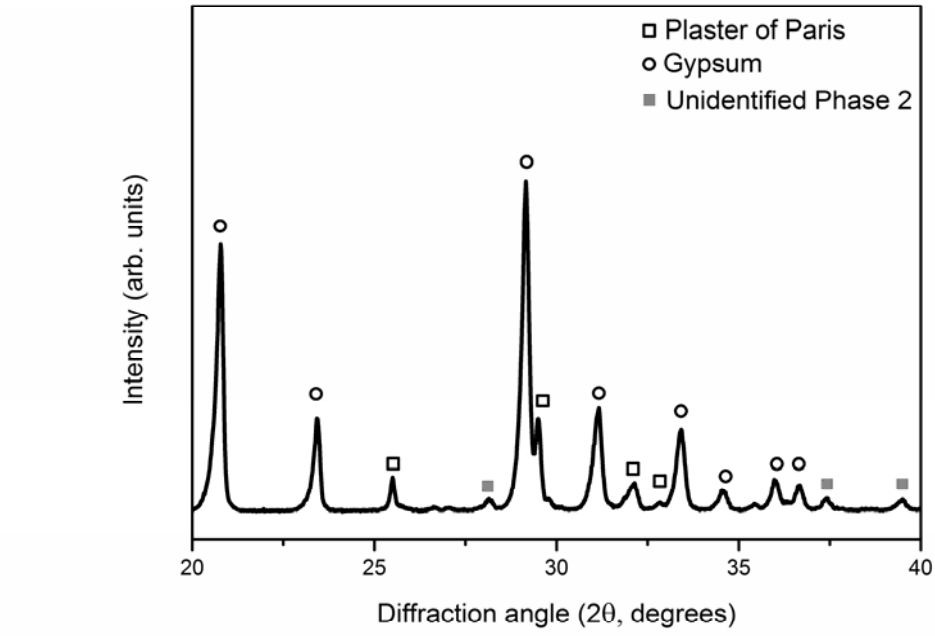

Figure 3.5 XRD diffractogram of bulk gypsum samples. As shown in the figure, some PoP remains after the setting reaction and complete conversion from PoP to gypsum is not achieved through hydration reaction.

shaped PoP to needle-like structured gypsum, which is typical for the hydration reactions. This change is expected to produce cement-type hardening. Between the needle-like features, there is intrinsic porosity introduced due to the hydration reaction. The SEM micrograph in Figure 3.7 shows the details of the microstructural features for this region. However, the porosity in this region seems to be much smaller compared to the macroporous regions in the perlite region. In Figure 3.6c (representative for region labeled as 2), the perlite region with high amount of porosity is shown. The porosity outside these regions is the air bubbles produced during mixing of the calcium sulfate powders with water.

Additionally, the regional chemical differences between gypsum and perlite regions were analyzed through EDS analyses and the results are shown by the spectra in Figure 3.8. EDS analyses showed that the region 1 shown on the SEM picture in Figure 3.6b is mostly calcium sulfate. On the other hand, the EDS analysis of the SEM picture in Figure 3.6c provided in Figure 3.8b. This figure reveals the presence of aluminum and silicon with calcium, suggesting presence of perlite phase in some form of alumina-silicate.

Finally, the density measurements were performed on the hydrated samples produced by changing the *s:l* ratio of the gypsum – water mixture. The *s:l* ratios and the level of porosity introduced by this method are shown in Table 3.2. The porosity values decreased by the increasing *s:l* ratio. These results are promising and suggesting that this approach can be used to modify/control porosity of the gypsum hydrated products.

Table 3.2 Porosity values of the bulk samples introduced by changing *s:l* ratio

Solid to Liquid Ratio (*s:l*)	**Porosity (*vol%*)**
1.33	54.5
1.67	51.8
2.22	47.8
3.33	39.4

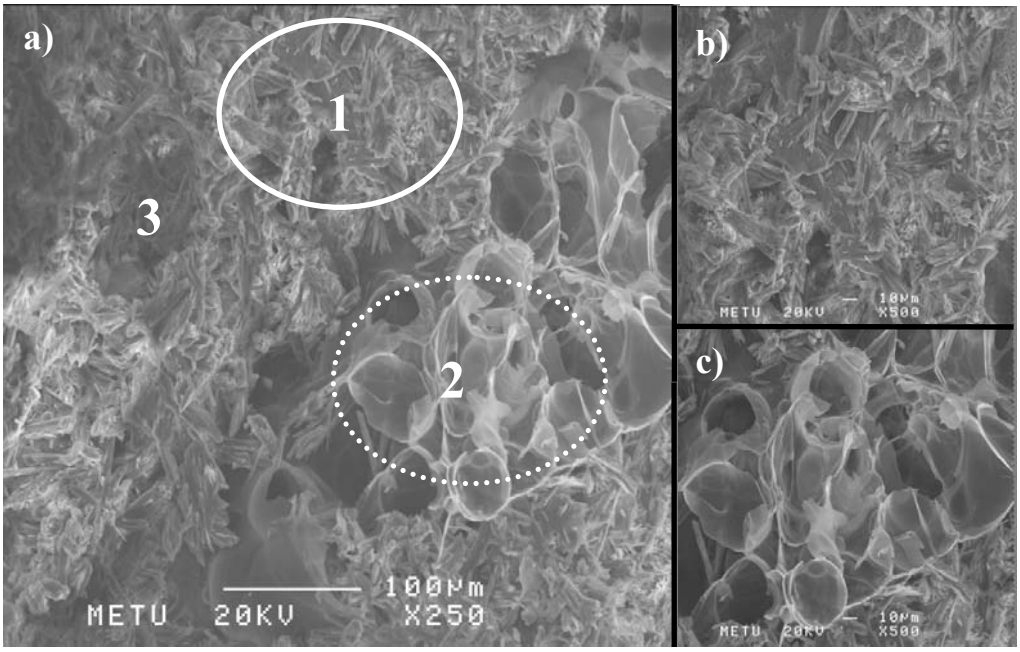

Figure 3.6 SEM micrographs of the sample produced through the hydration reaction of gypsum ($CaSO_4 \cdot 2H_2O$) from PoP ($CaSO_4 \cdot 0.15H_2O$) a) general view of the sample (250x magnification), b) Region 1 (calcium sulfate rich) (500x magnification), c) Region 2 (perlite rich) (500x magnification).

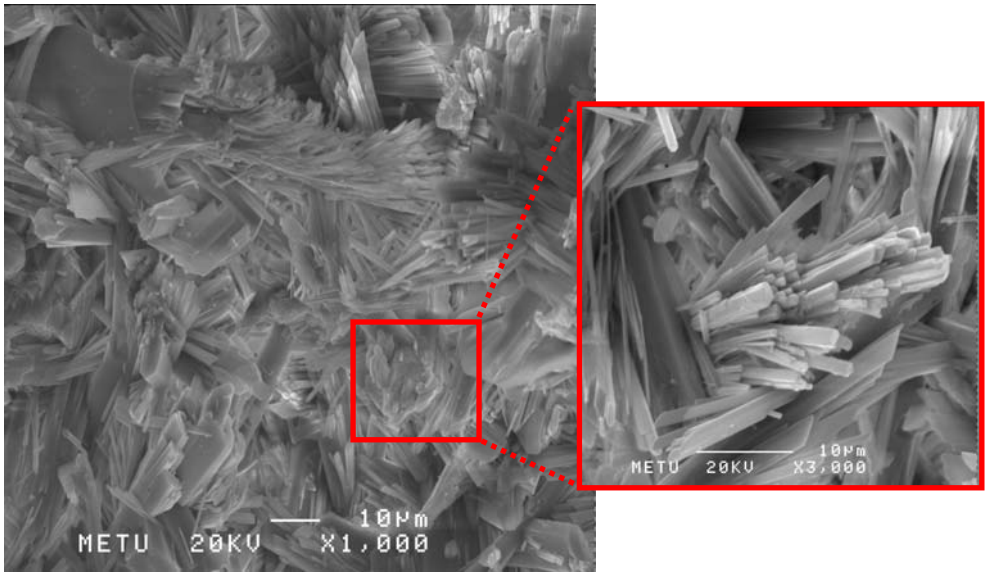

Figure 3.7 SEM micrographs showing the needle-like structure of the set gypsum in the bulk sample.

a)

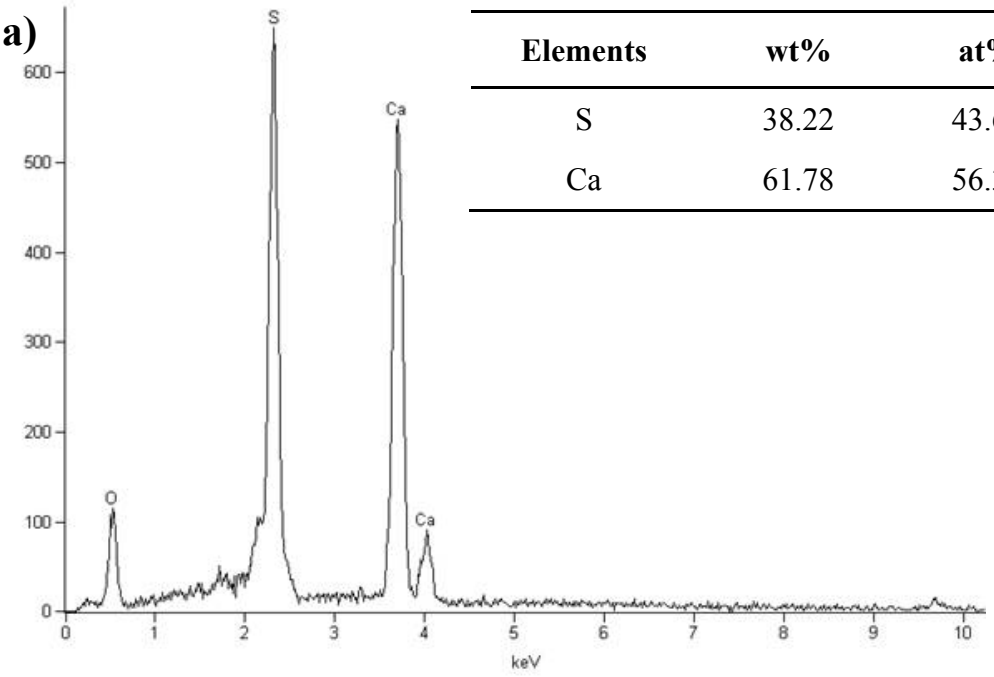

Elements	wt%	at%
S	38.22	43.61
Ca	61.78	56.39

b)

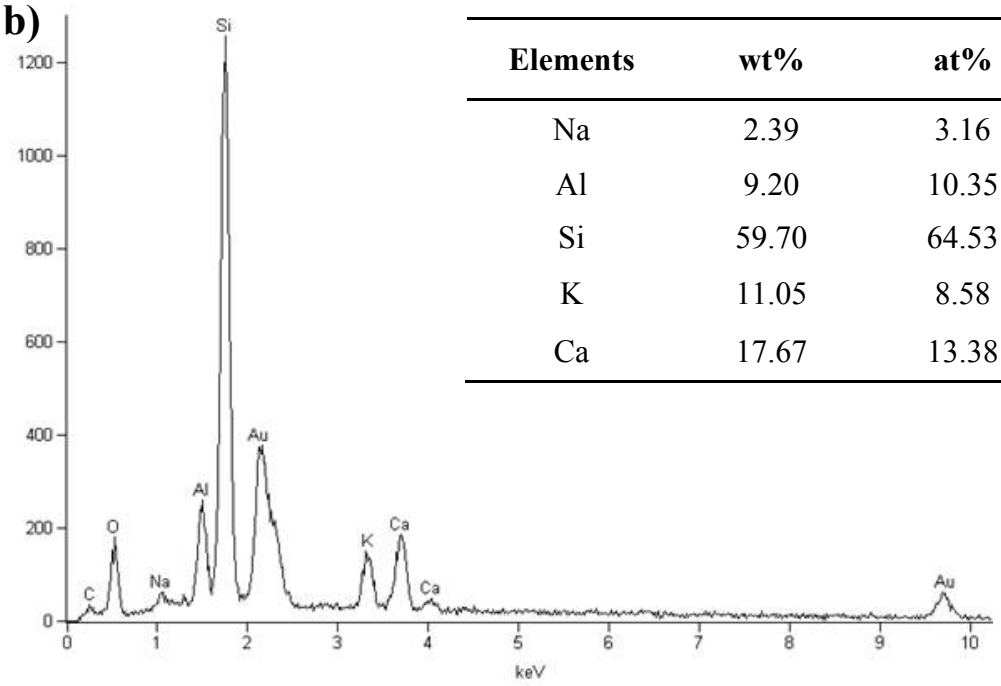

Elements	wt%	at%
Na	2.39	3.16
Al	9.20	10.35
Si	59.70	64.53
K	11.05	8.58
Ca	17.67	13.38

Figure 3.8 EDS spectra of a) calcium sulfate rich needle-like section and b) the perlite rich macroporous region (Au radiation is due to the conductive coatings used for SEM examination)

The SEM micrographs in Figure 3.9 do not reveal a significant difference for the bulk gypsum samples produced by different *s:l* ratios. The porosity created in perlite phase does not change while the *s:l* ratio changes. The porosity created by air bubbles seems to have nearly same size in all *s:l* ratios. Therefore, the main change on the porosity should be introduced by the calcium sulfate region. From these SEM micrographs, it is possible to observe that calcium sulfate region becomes more densely packed while the *s:l* ratio increases as revealed by the micrographs in Figure 3.9.

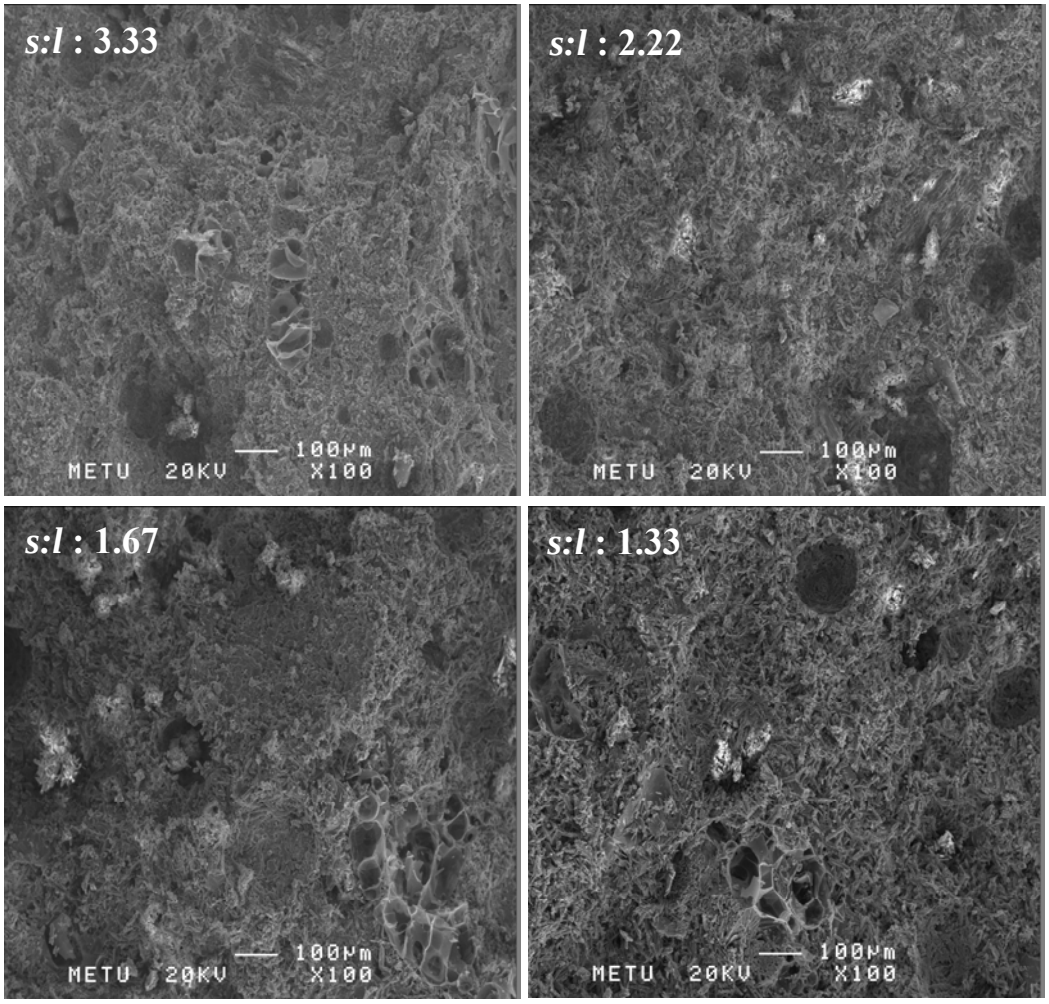

Figure 3.9 SEM micrographs of gypsum samples produced in different *s:l* ratios. Perlite region and porosity created by air bubbles do not differ by *s:l* ratio change, however needle-like gypsum part becomes looser by decreasing *s:l* ratio.

CHAPTER 4

RESULTS AND DISCUSSION - II

Assessments on conversion of calcium sulfates to HAp

In this part of the thesis, the reaction kinetics and the conversion process of different forms and types of calcium sulfates to HAp were analyzed using XRD and SEM examinations. This conversion process was performed in three different cases. These are the examinations of the *i)* conversion process from PoP powders to HAp powders, *ii)* conversion process from gypsum powders to HAp powders, and *iii)* conversion process of gypsum pellets to HAp. Schematic illustrations regarding to these studies are presented in Figure 4.1.

4.1. Conversion of PoP powders to HAp

4.1.1. Phase analyses of HAp powders synthesized from PoP

The synthesis experiments of HAp powders from PoP powders were conducted according to the methods explained in Section 2.2.2.1 and outlined by Figures 2.3 and 2.4. According to reaction 2.2, two routes were investigated to produce HAp powders from PoP powders. In route 1, experiments were conducted under ambient conditions. In this route, the samples were produced at room temperature (25 °C). The XRD diffractograms in Figure 4.2 show that the reaction product formed as a function of reaction time up to 21 days. After 7 days, the reactants have mostly converted into brushite ($CaHPO_4 \cdot 2H_2O$), a low temperature calcium

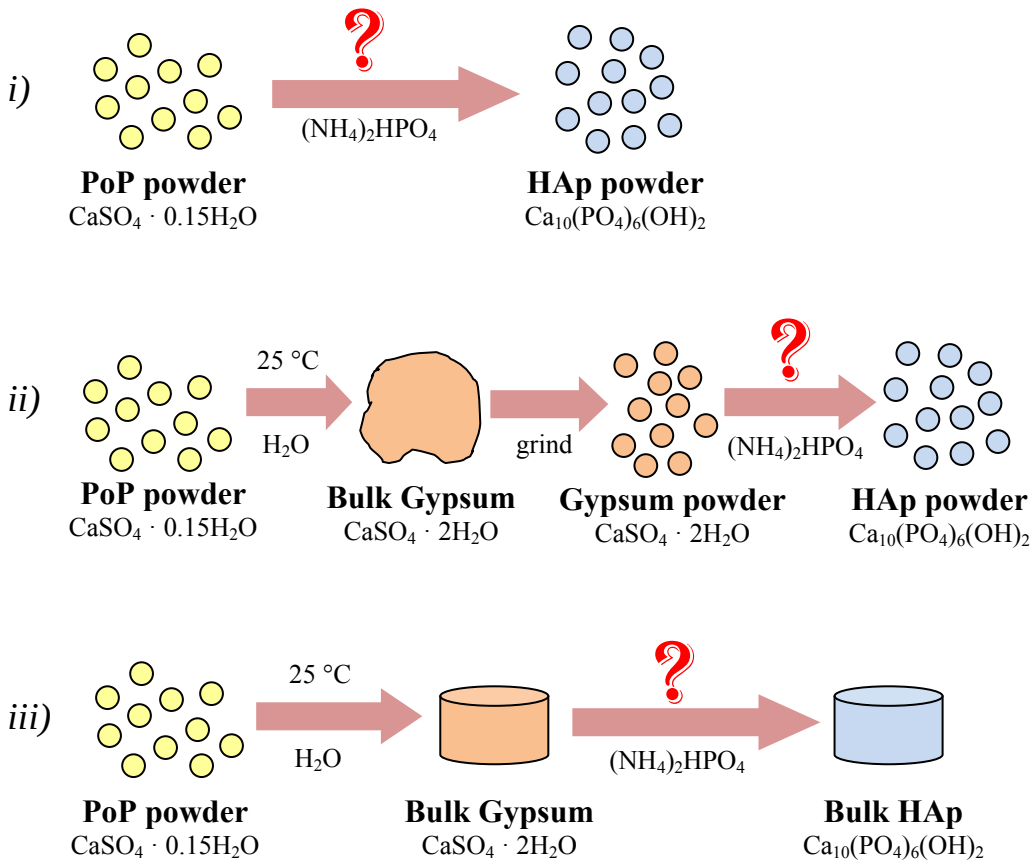

Figure 4.1 Schematic illustrations for the studies of the *i)* conversion process from PoP powders to HAp powders, *ii)* conversion process from gypsum powders to HAp powders, *iii)* conversion process of the bulk HAp from gypsum pellets.

phosphate phase with JCPDS card no. 09-077 and only a small amount of HAp (with the JCPDS card no. 09-432) was formed as identified by broad peaks at round 2θ of 31° - 33°. The unidentified phase (labeled as *Unidentified Phase 1*) coming from the calcium sulfate source seems to be eliminated during the reaction of PoP with $(NH_4)_2HPO_4$ solution.

The XRD diffractograms in Figure 4.3 shows that the reaction was not completed in 6 h at higher reaction temperatures, i.e. 50 °C. Additionally, an extra phase (labeled as *Unidentified Phase 3*) forms. This phase could be a calcium phosphate phase, however longer reaction times exceeding 6 h were not investigated.

Figure 4.4 shows the XRD diffractograms of the conversion reactions performed at 90 °C. According to this figure, the reaction seems to be more complete compared those reactions performed at 25 °C and 50 °C, as the characteristic HAp diffraction peaks (2θ ≈ 31° - 33°) can be more clearly observed even after 2 h of reaction. As the reaction period was extended from 2 h to 6 h, the HAp product becomes more crystalline and peaks becomes more distinct. The extra phase (labeled as *Unidentified Phase 4*) is still present and acting in a random manner, which is an unexpected and unexplained situation. But, the detailed investigation/identification of these unknown phases has been considered trivial within the general scope of the thesis. These phases constitute a very small portion of the product.

In route 2, as outlined in Figures 2.3 and 2.4, the effect of pressure on the PoP to HAp conversation kinetics was examined. The pressure and temperature were set to a constant value of 2 ± 0.2 atm and 120 °C, respectively. Due to these specific limits of the pressure chamber employed in the experiments, the pressure and the temperature variable cannot be studied systematically for pressurized experiments. Additionally, in this route, the effect of changing chemical composition and the effect of washing on HAp products were studied, in an effort to eliminate the unidentified phases that form during reaction of PoP powder with $(NH_4)_2HPO_4$ solution.

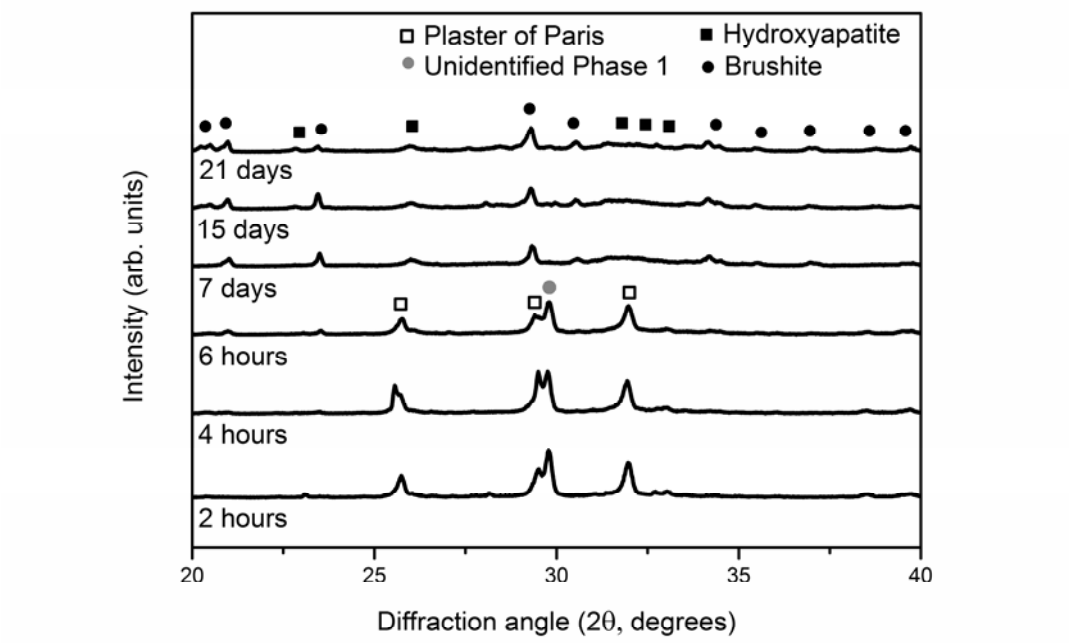

Figure 4.2 XRD diffractograms of the products converted from PoP by using 1 M of $(NH_4)_2HPO_4$ conducted at 25 °C and under ambient conditions. After 7 days, calcium sulfate powders were converted into brushite ($CaHPO_4 \cdot 2H_2O$), and only a small amount of HAp was formed**.**

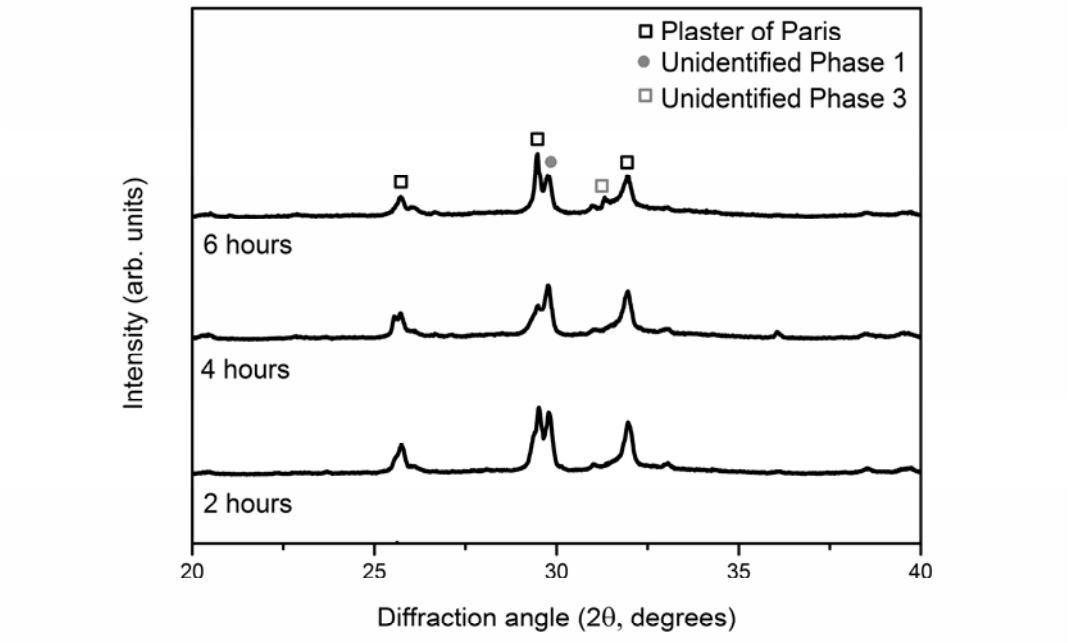

Figure 4.3 XRD diffractograms of the products converted from PoP by using 1 M of $(NH_4)_2HPO_4$ conducted at 50 °C and under ambient conditions. At this temperature, conversion was not achieved after 6 hours, instead a new unidentified phase was formed.

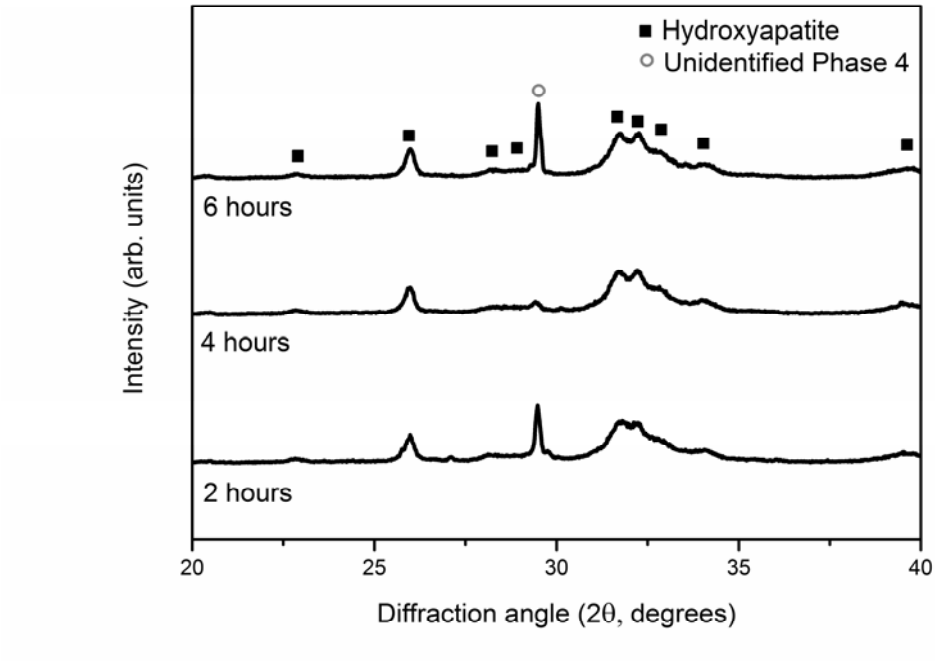

Figure 4.4 XRD diffractograms of the products converted from PoP by using 1 M of $(NH_4)_2HPO_4$ conducted at 90 °C and under ambient conditions. The conversion reaction seems to be more successful than the reactions at 25 °C and 50 °C. Additionally, as the reaction time increases, produced HAp becomes more crystalline. However, the unidentified phase acts randomly with the reaction time.

The kinetic study of the reaction was done in the pressure vessel using, again, 1 M of $(NH_4)_2HPO_4$. The reactions lasted from 15 min up to 1 h in 15-minute intervals, from 1 h to 2 h in 30-minute intervals, from 2 h to 6 h in 2-hour intervals. Additionally, a 12-hour experiment was performed. The XRD diffractograms in Figure 4.5 show that in 15 minutes the conversion to HAp starts and in 30 minutes, more HAp is produced compared to 15-minute reaction the remainder phase being unreacted PoP. In 30 minutes up to 90 minutes, PoP was still present in the sample. After 2 hours, the reaction seems to be complete to some extent. As reaction time increases, crystallinity of the HAp phase enhances, but the highly crystalline HAp phase could not be obtained from these reactions. The produced HAp is identified by the broad characteristic peaks at $2\theta \approx 31° - 33°$. Additionally, the extra phase (labeled as *Unidentified Phase 1*) converts into some other phase (labeled as *Unidentified Phase 4*) as reaction time increases. The intensity of the extra phase apparently reduces with time; however it is impossible to say that it can be eliminated at longer reaction times due to the uncertain behavior of these phases. The new unidentified extra phase also does not match with any standard JCPDS card.

The effect of washing of the conversion products (HAp powders) using DI-water was examined in order to inspect the chemical stability of the products. In addition, some unstable or water-soluble residues can be removed by washing. Since, the starting materials are fairly impure, the effect of washing becomes an important factor. Figure 4.6 shows the XRD diffractograms for pre- and post-washing processes of the HAp samples produced by hydrothermal-like conditions after 2 h, 4h and 6 h from 1 M of $(NH_4)_2HPO_4$ solution. Washing with DI-water does not influence HAp phase, however some additional unidentified phases are formed. This means that HAp phase is stable and does not dissolve in water, exhibiting certain crystallinity. However, washing does not eliminate the unidentified phase (labeled as *Unidentified Phase 4*) and in fact, one additional extra phase is formed (labeled as *Unidentified Phase 6*).

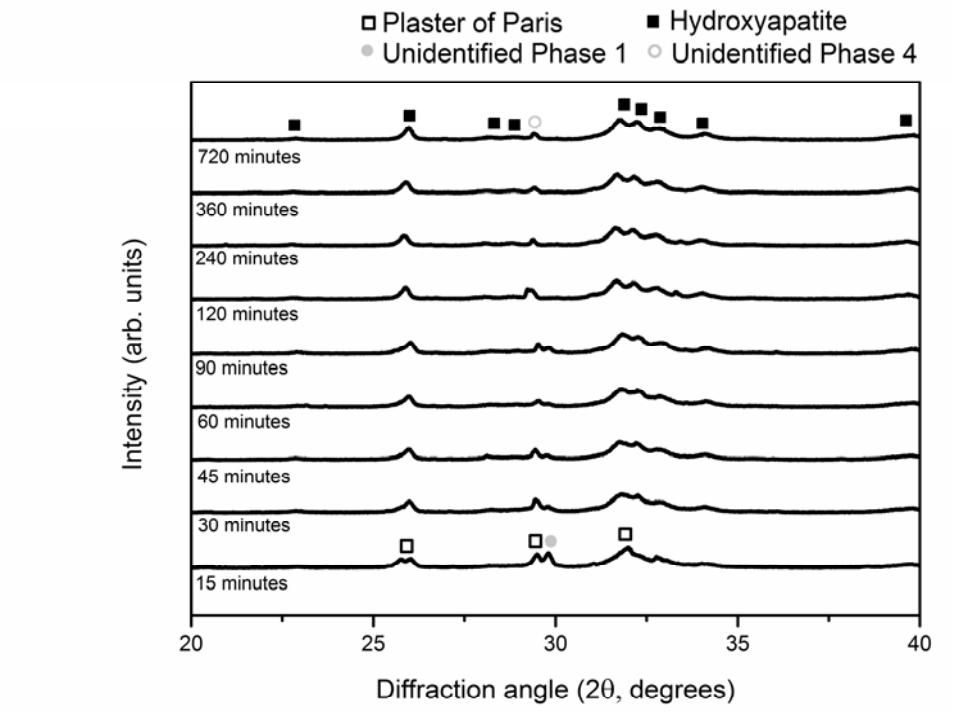

Figure 4.5 XRD diffractograms of the products converted from PoP powders using 1 M of $(NH_4)_2HPO_4$ solution under hydrothermal-like conditions (120 °C and 2 ± 0.2 atm). The reactions lasted from 15 min to 12h. As shown in the figure, HAp conversion can be achieved in 15 min., however increase in reaction time also increases the crystallinity of the HAp.

a)

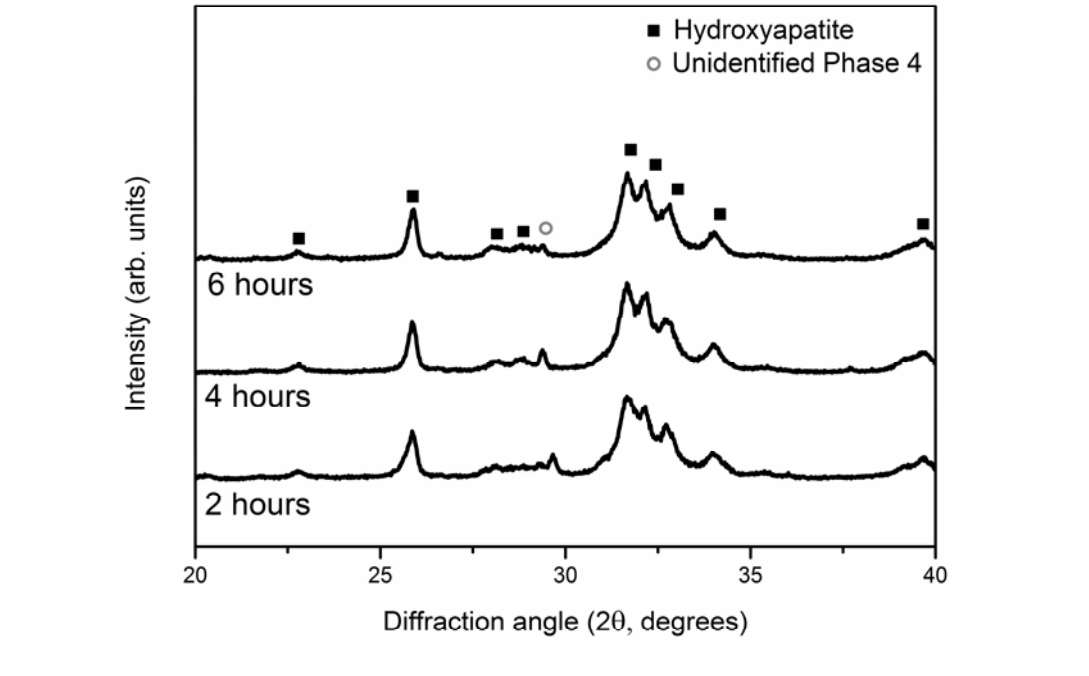

b)

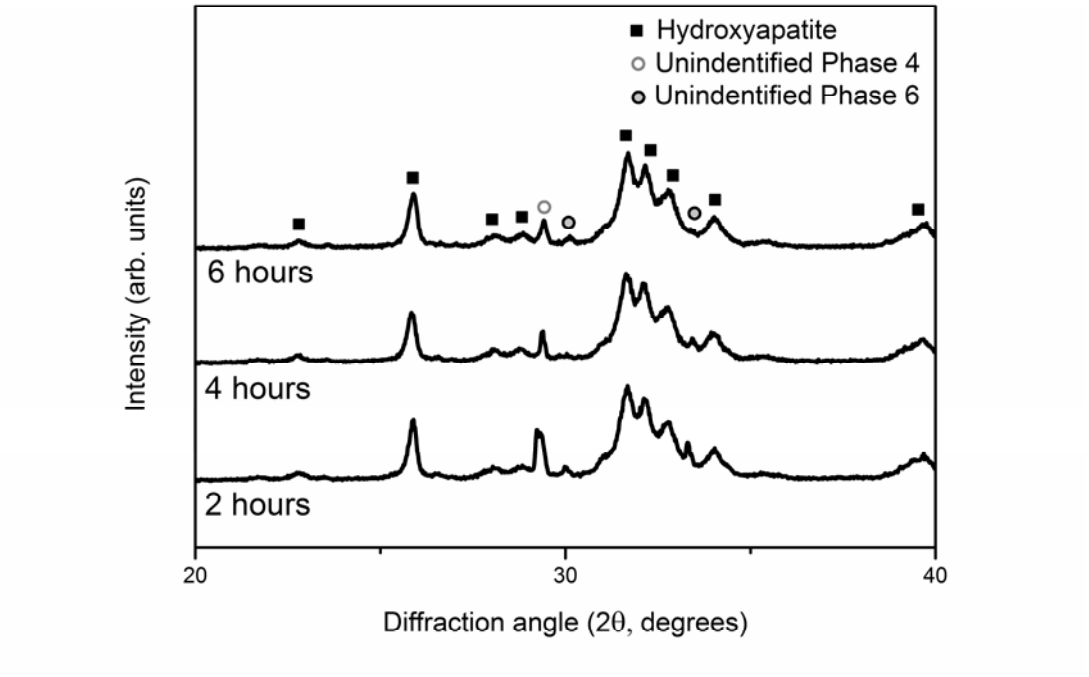

Figure 4.6 XRD diffractograms of the products formed using 1 M of $(NH_4)_2HPO_4$ solution, a) before washing and b) after washing under hydrothermal-like conditions (120 °C and 2 ± 0.2 atm). As shown in the figure, washing influences the occurrence of unidentified phases, however there is no change observed on the HAp phase.

The XRD diffractograms for pre- and post-washing processes of the HAp samples produced by hydrothermal-like conditions after 2 h, 4h and 6 h from 0.5 M of $(NH_4)_2HPO_4$ solution are shown in Figure 4.7. According to this figure, washing with DI-water affects the HAp powders positively compared to previous results. During washing, the remaining PoP phase is nearly removed due to high solubility of PoP in water. However, additional extra phases (labeled as *Unidentified Phase 5*) were formed during washing. One important finding related with the washing operation was the observation of the change in the crystallinity of the samples. After washing operation, HAp powders seem to have higher crystallinity compared to pre-washed samples.

Figure 4.6 and 4.7 also showed that conversion process is positively related with the molarity of $(NH_4)_2HPO_4$ solution. HAp produced using 0.5 M of $(NH_4)_2HPO_4$ solution seems to have more distinctive peaks, however the reaction period should be longer than 6 h in order for complete conversion of PoP powders to HAp. HAp produced using 1 M of $(NH_4)_2HPO_4$ solution have more intimate peaks, as the reaction time increases the peaks became more distinctive. As discussed in the study of Furuta et. al [24], 1 M of $(NH_4)_2HPO_4$ solution affects the reaction kinetics in a positive manner, increasing its rate. They claimed that 1 M of $(NH_4)_2HPO_4$ solution was interacted with PoP very quickly, and an impervious layer of HAp was produced on the surface of the prismatic PoP particles. Consequently, the interior side of PoP particles was not reacted due to the lack of diffusion through the layer of relatively dense HAp products. They also stated that using 0.5 M of $(NH_4)_2HPO_4$ solution would make the reaction slower, but more efficient with respect to the experiments performed using 1 M of $(NH_4)_2HPO_4$ solution. As a result of slow and more gradual reaction kinetics, the reactant solution would diffuse through the center (core) of the PoP particles before the formation of excessive deposit of HAp layer on the surface of the prismatic particles.

a)

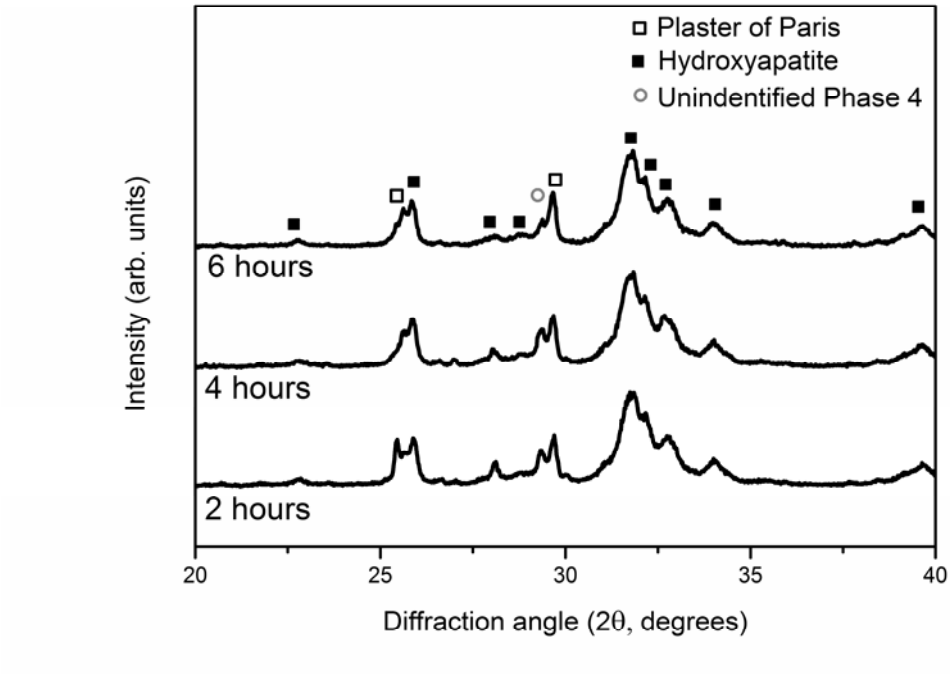

b)

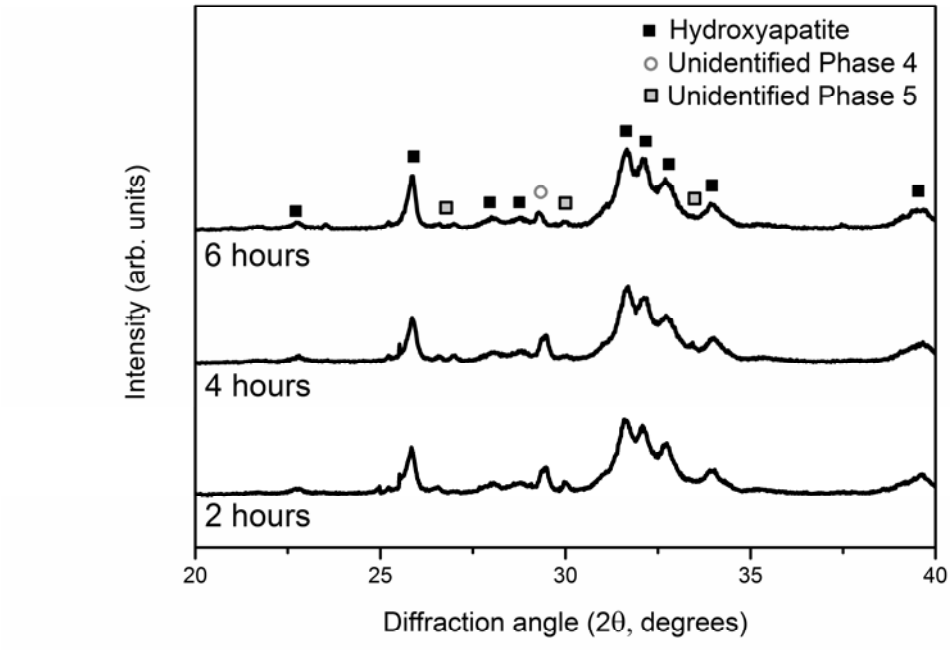

Figure 4.7 XRD diffractograms of the products formed using 0.5 M of $(NH_4)_2HPO_4$ solution, a) before washing and b) after washing under hydrothermal-like conditions (120 °C and 2 ± 0.2 atm). As shown in the figure, washing influences the occurrence of unidentified phases, however there is no change observed on the HAp phase

4.1.2. Morphological analysis of HAp powders synthesized from PoP

The SEM micrographs in Figure 4.8 show the morphological details of the HAp powder samples obtained from PoP powders. These figures show the micrographs of HAp produced using 1 M of $(NH_4)_2HPO_4$ solution for 2 h, 4 h and 6 h reaction time. According to this figure, the morphology of the particles has changed compared to their initial appearance shown in Figure 3.2. The new form resembles the general prismatic structure of the α-hemihydrate; however, the surface of these prismatic particles is covered with newly formed HAp crystals. It is impossible to predict the chemical composition of the interior side (core) of the particles; however, XRD data has shown that almost complete conversion to HAp has occurred. Newly formed HAp on the surface of the PoP particles has needle-like morphology with an approximate crystal size of 1 to 8 μm. The details on microscopic change can be seen by the SEM micrograph in Figure 4.9. It is possible to clearly observe the reticulated needle-like crystals of HAp with a primary particle size of 20 – 30 μm. The needle-like structure was also observed in the study of Furuta et. al [24]. #

Additionally, EDS spectra of the produced HAp powders shown in Figure 4.10 give some insights about the chemical nature of the reaction products obtained by hydrothermal-like conditions**.** According to the EDS spectra, Ca/P ratio increases from 1.33 to 1.67 while the reaction time increases from 2 h to 6 h. Even though, exact chemical composition analyses based solely on EDS data are questionable, these data, at least, show qualitatively that the reaction products forming in early stages are calcium-deficient. However, after prolonged and efficient reaction with $(NH_4)_2HPO_4$ solution, stoichiometric $Ca_{10}(PO_4)_6(OH_2)$ with Ca/P ratio of 1.67 can be produced with the hydrothermal-like reactions.

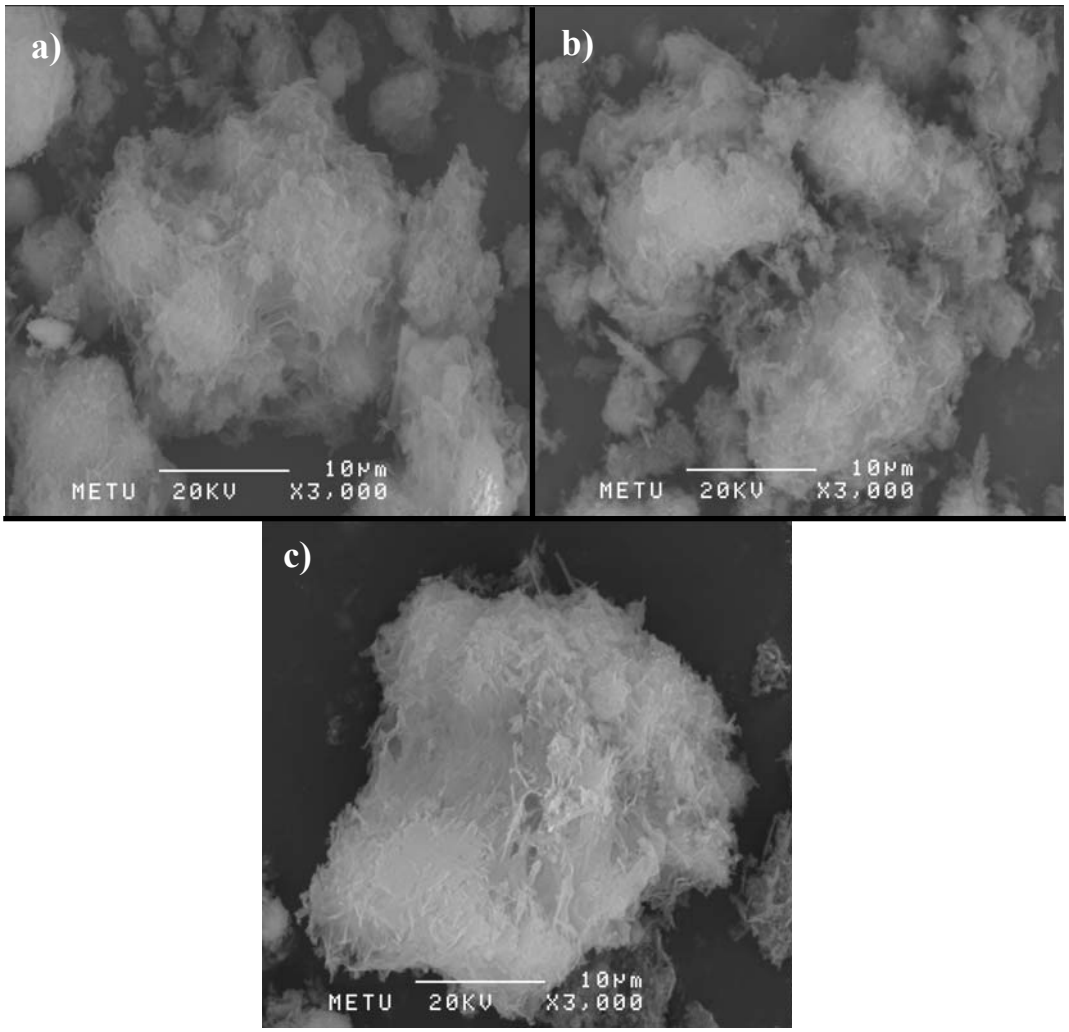

Figure 4.8 SEM micrographs of HAp powder samples produced under hydrothermal-like conditions (120 °C and 2 ± 0.2 atm) and using 1 M of $(NH_4)_2HPO_4$ solution for a) 2 h, b) 4 h, c) 6 h reaction time. HAp was produced under these conditions; however it is not possible to observe considerable change on these micrographs. (Magnification: 3000x)

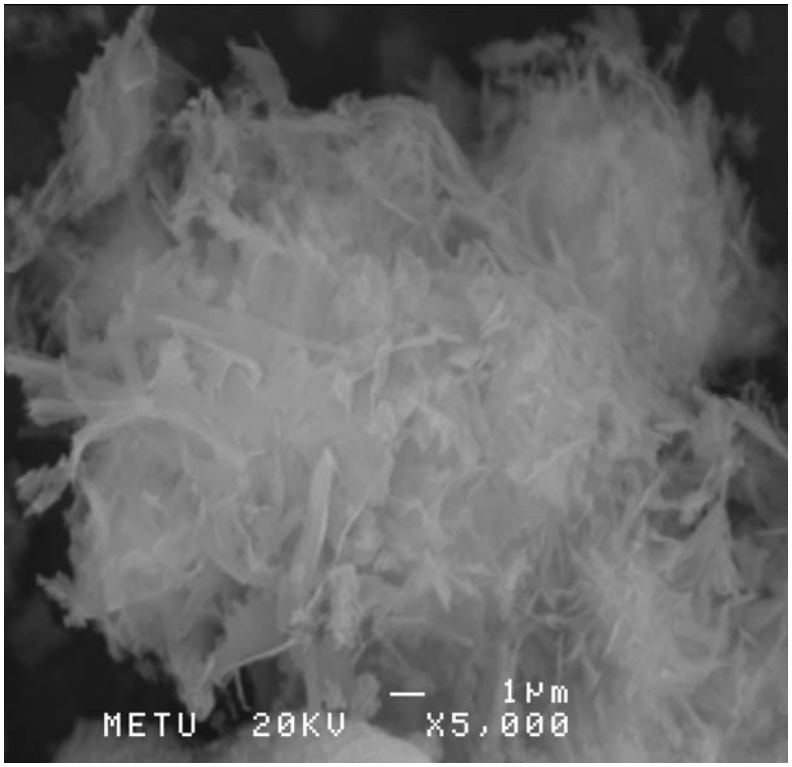

Figure 4.9 SEM micrograph of the HAp produced using 1 M of $(NH_4)_2HPO_4$ solution for 4 h reaction time under hydrothermal-like conditions (120 °C and 2 ± 0.2 atm) showing the HAp crystals with needle-like morphology with a crystal size of 1 μm to 8 μm. (Magnification: 5000x)

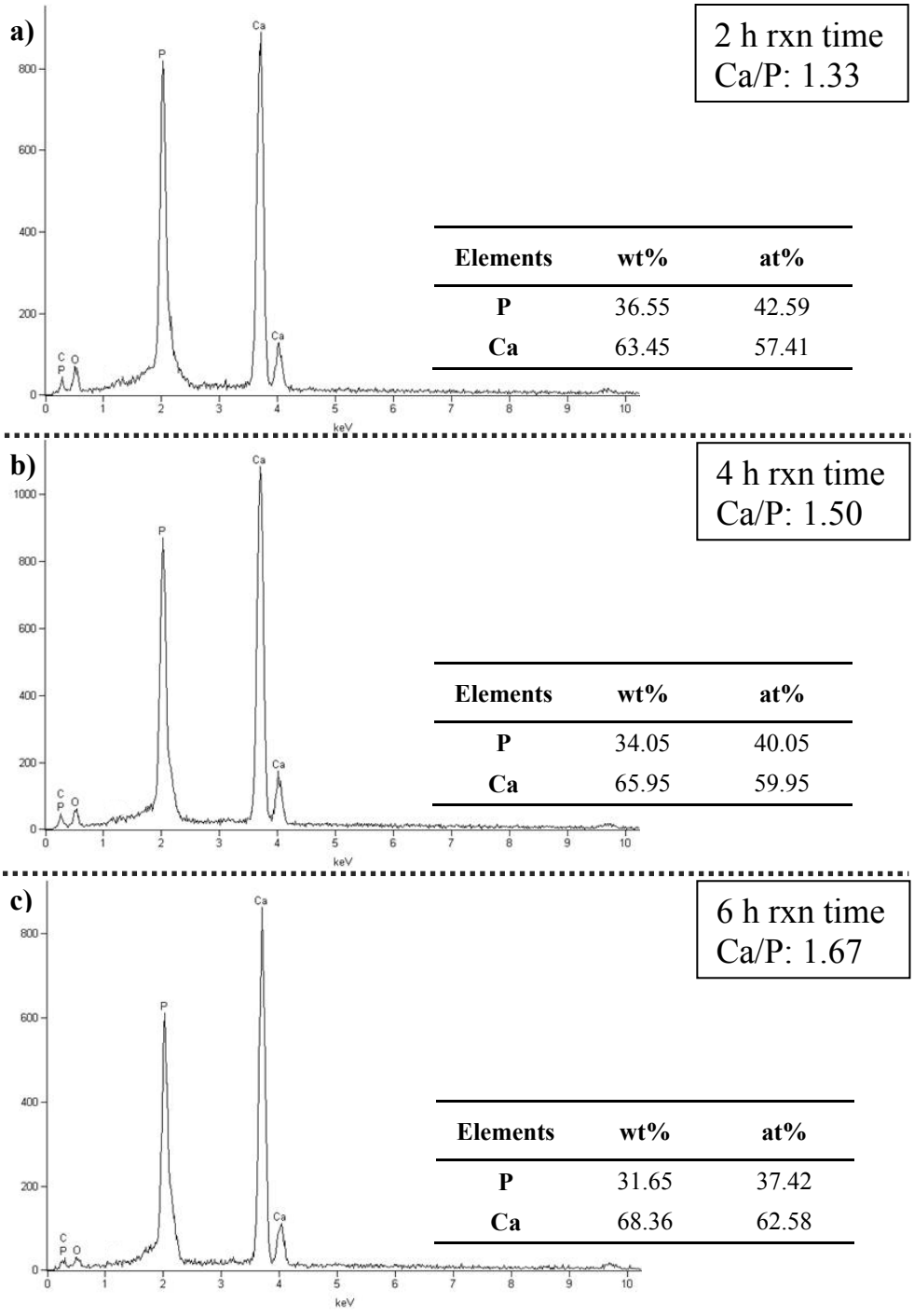

Figure 4.10 EDS spectra of HAp produced using 1 M of $(NH_4)_2HPO_4$ solution for a) 2h, b) 4 h, c) 6 h reaction time. Determined Ca / P ratios are 1.33, 1.50 and 1.67 respectively.

4.2. Conversion of gypsum powders to HAp

In this part of the thesis, gypsum powders were used as precursor for HAp conversion. As illustrated in Figure 2.5, PoP powders were first mixed with DI-water using an *s:l* ratio of 1.67 and the sample was dried for one day at 25 °C. After drying, the sample was grinded using an agate mortar and pestle, and these powders were used in the following experiments on conversion to HAp. Typically, the samples were reacted using 1 M of $(NH_4)_2HPO_4$ solution for 6 h in the pressure cooker. Finally, the products are washed with DI-water and dried at 75 °C. Characterization on these samples was performed using XRD.

Figure 4.11 shows XRD diffractograms of the conversion product for the comparison purposes, showing the difference for the HAp produced from PoP and gypsum powder precursor under hydrothermal-like conditions. The diffractograms show that conversion to HAp was successful in both powder precursors. The HAp product synthesized from PoP powders seems to be more crystalline than the product synthesized from gypsum powders. This result suggests that anhydrate form of the calcium sulfate precursor (PoP) is more reactive than the hydrated form of the calcium sulfate precursor (gypsum) in terms of conversion to HAp. The possible reason for relatively the poor crystalline HAp product of gypsum-employed studies may be the difference in wetting properties due to initial hydration with water of in before reacting gypsum with $(NH_4)_2HPO_4$ solution. As also seen in the previous XRD results, the extra phase is still present for the product obtained from PoP. This phase does not match with any standard JCPDS card. However; this extra phase was absent when gypsum powders were used in the reactions.

4.3. Conversion of bulk gypsum pellets to HAp

The HAp produced from gypsum pellets were also investigated. These investigations are compared with the results of HAp obtained from the reaction

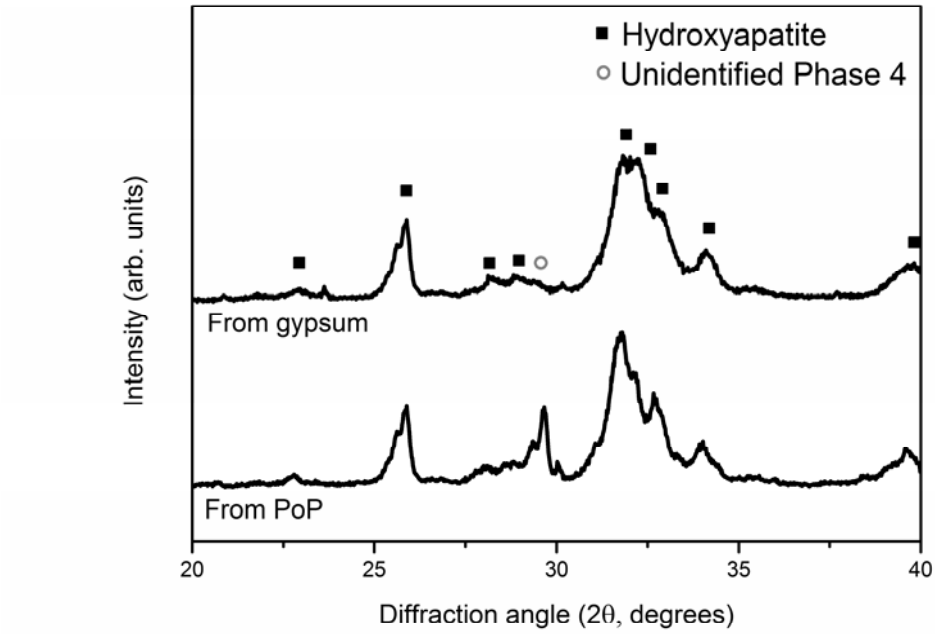

Figure 4.11 A comparison of XRD diffractograms of the HAp samples produced from PoP powders (before hydration) and gypsum powders (hydrated with DI-water, dried at 25 °C and grinded to obtain powder form) after 6 h reaction. It is possible to investigate that using PoP powders as a precursor for HAp production results more crystalline phase of the product (HAp) compared to the gypsum precursor, even though both precursors are in powder form.

with gypsum powder precursors. As illustrated in Figure 2.8, the bulk samples were firstly hydrated with DI-water in varying *s:l* ratios and dried at 25 °C for one day. After drying operation, all samples were reacted with 1 M of $(NH_4)_2HPO_4$ solution for 6 h in pressure vessel. Finally, the products were washed with DI-water and dried at 75 °C for one day. Characterization on these samples was performed using XRD and SEM.

4.3.1. Phase analyses of bulk HAp synthesized from gypsum pellets

In Figure 4.12, the XRD data for the conversion products produced from bulk form of gypsum with an *s:l* ratio of 1.67 and powder form of the gypsum are shown for comparison purposes. In both cases, complete transformation to HAp was

achieved; however an extra unidentified phase (labeled as *Unidentified Phase 4*) is present in both products. The product of bulk gypsum has more well defined diffraction peaks compared to the product of powder form of gypsum, meaning that HAp product of gypsum powder is more crystalline compared to the product of its bulk counterpart. Both products are poorly crystalline compared to those in the previous work (i.e. Figure 4.5). Longer reaction times could be investigated to observe for the crystallinity increase of the resultant products in addition to the removal of unidentified phase (labeled as *Unidentified Phase 4*), but was not accomplished in this work.

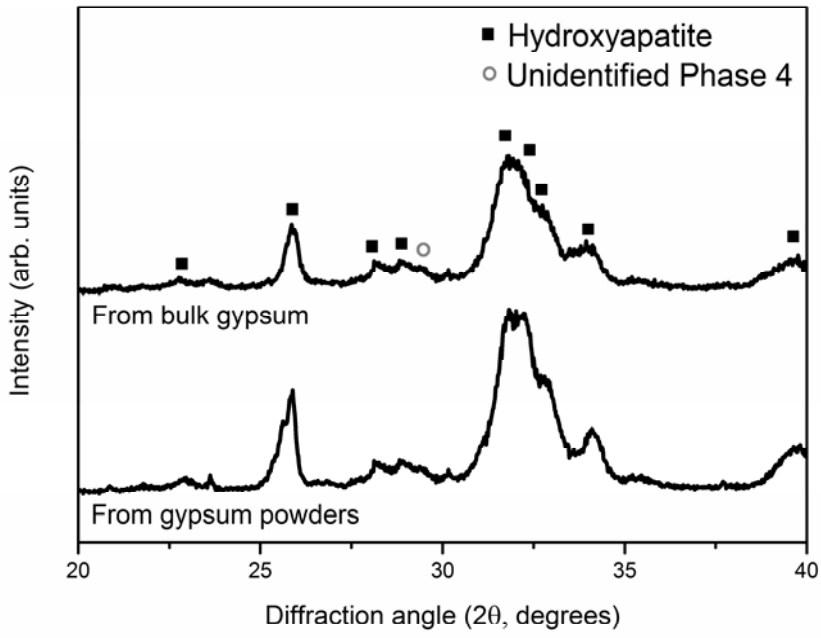

Figure 4.12 A comparison of XRD diffractograms of the HAp samples produced from bulk and powder forms of gypsum after 6 h reaction. HAp produced from powder form of gypsum has more distinctive peaks compared to the HAp produced from bulk form.

4.3.2. Morphological analyses of bulk HAp pellets synthesized from gypsum pellets

SEM micrographs of the bulk HAp pellets with *s:l* ratios of 3.33, 2.22, 1.67 and 1.33 are shown in Figure 4.13 and Figure 4.14. Recalling the SEM micrograph of Figure 3.6 as the micrographs share the same aspects (calcium rich region, perlite rich region and air bubbles). The calcium rich region was completely converted into HAp, and in addition, the perlite rich region was partially covered with HAp also. Air bubbles seem to contain the same size compared to region 3 of the Figure 3.6. The details of the HAp conversion in bulk state were shown in Figure 4.14. As shown in the figure, HAp was produced as spherical crystals in *s:l* ratio of 3.33. While the *s:l* ratio decreases, needle-like crystals form. For *s:l* ratio of 1.33, the crystal size seems to be the smallest, in addition to the needle-like structure, in compared to other *s:l* ratios. This type of morphology was also observed in the study of Lowmunkong et. al. [27].

The porosity data of the pre- and post-reaction state of the bulk samples are shown in Table 4.1. The porosity increases drastically after the conversion reaction. The porosity increase on the pellets having *s:l* ratio of 1.33, 1.67, 2.22 and 3.33 are 34.1, 39.0, 44.4 and 55.1 vol%, respectively. The final porosity of the HAp structures increases with *s:l* ratio.

Table 4.1 Porosity values of the bulk gypsum pellets (before conversion reaction) and the bulk HAp samples (after conversion reaction) introduced by changing *s:l* ratio.

Solid to Liquid Ratio (*s:l*)	**Porosity of bulk gypsum (*vol%*)**	**Porosity of bulk HAp (*vol%*)**
1.33	54.5	73.1
1.67	51.8	72.0
2.22	47.8	69.0
3.33	39.4	61.1

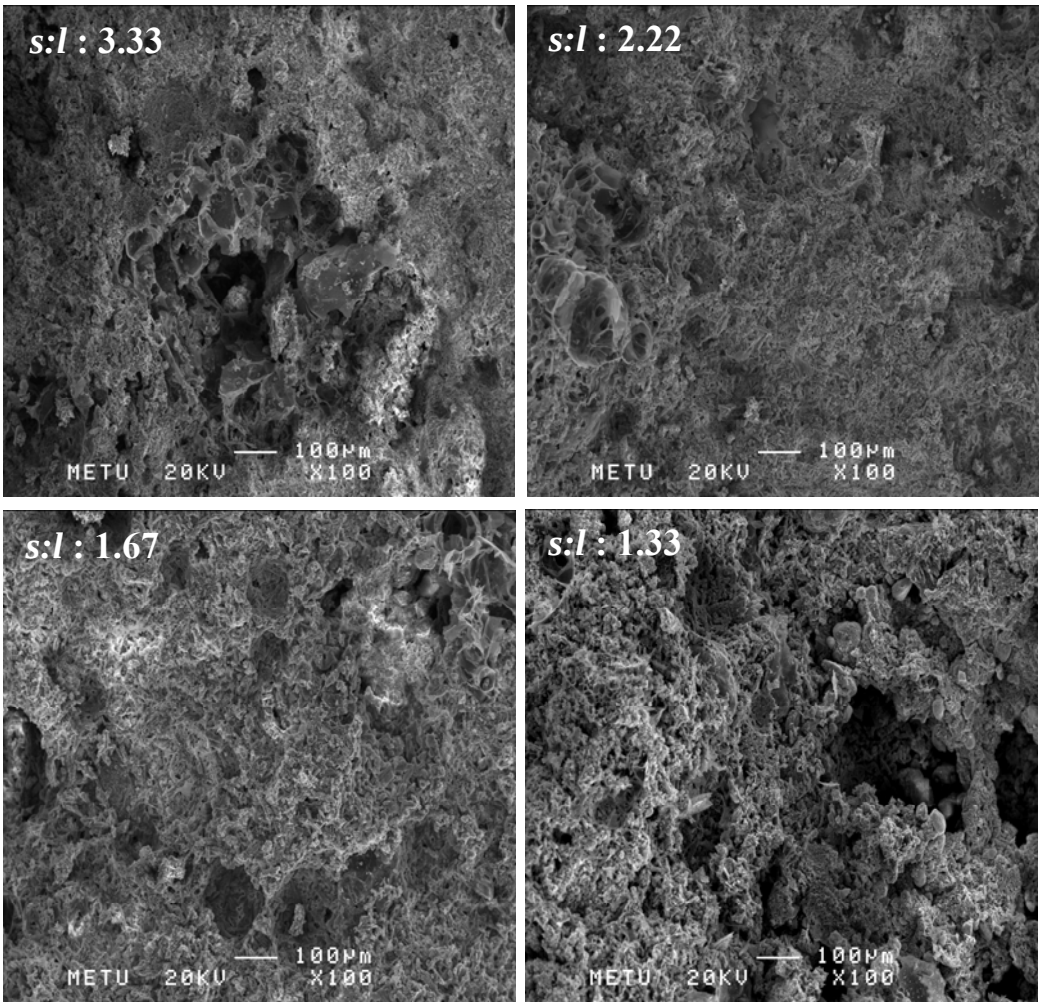

Figure 4.13 SEM micrographs of the conversion products produced from gypsum pellets with different *s:l* ratios (100x magnification). All figures contain the main aspects considered in Figure 3.6, additionally calcium sulfate rich regions were fully converted to HAp. Moreover, HAp was also observed in perlite rich regions.

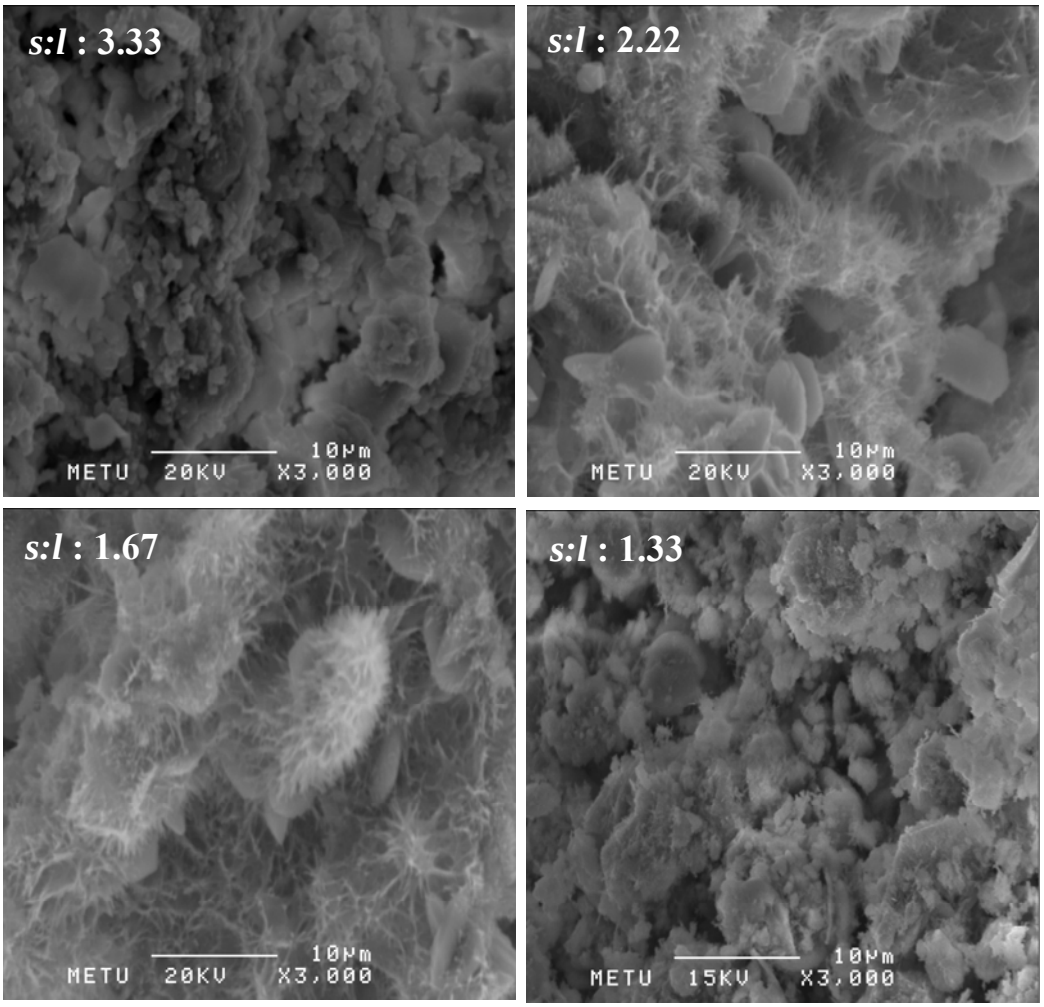

Figure 4.14 SEM micrographs of the conversion products (HAp) produced from gypsum pellets with different *s:l* ratios (3000x magnification). In the most compact structure (with *s:l* ratio of 3.33) HAp was produced as spherical crystals, however while the compaction ratio decreases (the *s:l* ratio decreases), needle-like crystals has began to occur on the spherical structures.

CHAPTER 5

RESULTS AND DISCUSSION – III

Additional characterization studies of the conversion products: HAp

5.1. Exact chemical identity of the HAp products

In this part of the thesis, exact chemical identity of the synthesized HAp powders was studied. The phase changes upon heating can be related to the chemistry and stoichiometry of the HAp, i.e Ca/P atomic ratio, with the help of $CaO\text{-}P_2O_5$ phase diagram shown in Figure 5.1 [40].

The heat treatment experiments were applied to HAp products of 30- minute and 6-hour hydrothermal-like conversion reactions of PoP powders. The HAp products were calcined in the temperature range of 200 °C to 1200 °C. After the heat treatment operation, the samples were air cooled to room temperature (25 °C). Characterization of these samples was performed using XRD analysis.

The XRD diffractograms in Figure 5.2 show the phase changes for 30-min and 6-h reacted HAp powders upon heating at 1200 °C. As seen in the figure, regardless of the reaction time, the HAp products were found to be stable up to 600 °C. Beyond 800 °C, HAp converts into β-tricalcium phosphate (β-TCP). While the heat treatment temperature increases, the crystallinity of the β-TCP phase increases. Additionally, the extra phase (labeled as *Unidentified Phase 4*) seems to be eliminated after the heat treatment operation at 800 °C.

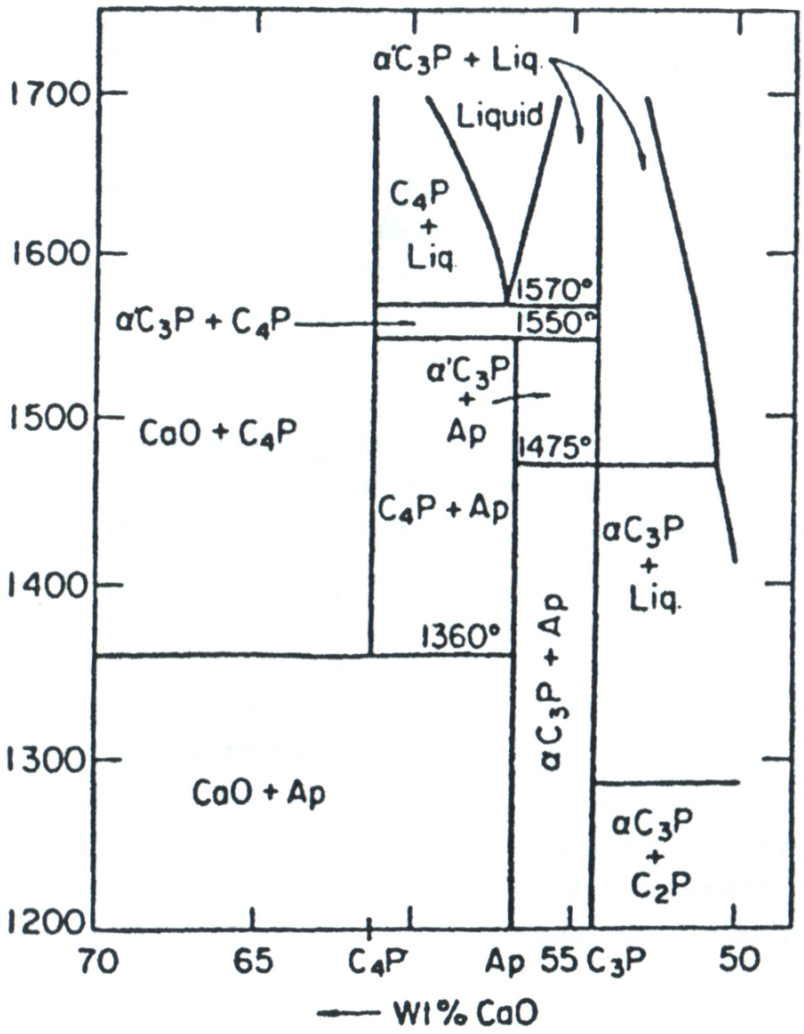

Figure 5.1 Phase diagram of CaO-P_2O_5 system (C: CaO, P: P_2O_5) showing stoichiometric HAp (abbreviated as "Ap") phase (Ca/P: 1.67)

The formation of β-TCP shows that the products have Ca/P ratio between 1.50 and 1.67 which means the products are calcium deficient. HAp with exact stoichiometric Ca/P ratio of 1.67 should be stable up to 1550 °C (according to the phase diagram in Figure 5.1) which incongruently melts at this temperature. However, recalling the previous EDS data, the products should have a Ca/P ratio smaller than 1.67, but in close proximity to this value.

According to the phase diagram of $CaO\text{-}P_2O_5$ system in Figure 5.1, α-TCP is stable at high temperatures (higher than 1100 °C) and in order to produce α-TCP phase, the reactants should be quenched to room temperature (25 °C) after heat treatment. Moreover, β-TCP phase is stable at 25 °C and it can be produced by air cooling of the HAp after heat treatment. As previously mentioned, in the experiments throughout this thesis work, always excess amount of phosphate source was used. This was done in order to achieve complete wetting of the PoP/gypsum powders and pellets. So the resulting HAp was found to be Ca-deficient as suggested earlier by EDS analyses and proven by the qualitative evaluations performed in this section.

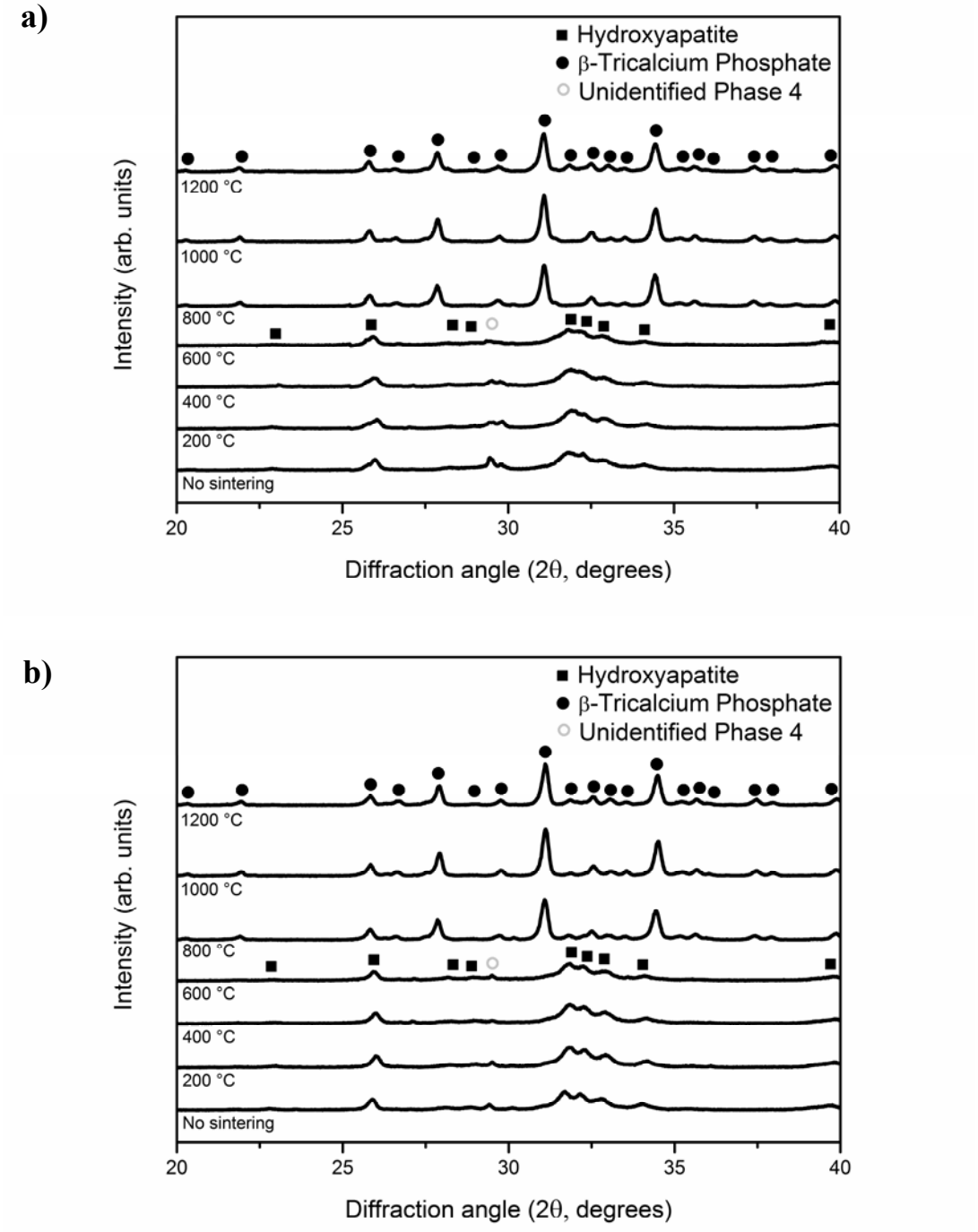

Figure 5.2 XRD diffractograms of the heat treated HAp powders converted from PoP powders under hydrothermal-like conditions after a) 30 min reaction, and b) 6 h reaction. The samples are sintered for 2 h after the conversion process. As seen in the figure, HAp phase is stable up to 600 °C and after 800 °C; HAp was fully converted into β-tricalcium phosphate (β-TCP).

5.2. Mechanical properties of the bulk HAp and HAp/PCL composites

In this part of the thesis, mechanical properties (fracture strength) of bulk HAp and HAp/polycaprolactone (abbreviated as HAp/PCL) composites are reported. First, the mechanical properties of gypsum pellets of different *s:l* ratio were measured. This set of samples exhibit different porosity values as shown earlier studies. Typically, the set pellets dried for 1 day at 25 °C. Then, these gypsum pellets were reacted 6 h with 1 M of $(NH_4)_2HPO_4$ solution under hydrothermal-like conditions and converted to bulk HAp pellets. The conversion products (HAp pellets) were dried for 1 day at 75 °C and these samples were used in diametrical compression tests.

The results of the mechanical strength evaluations are shown in Table 5.1. The fracture strengths of the HAp pellets having an initial *s:l* ratio of 1.33, 1.67, 2.22 and 3.33 are found as 0.3 MPa, 0.5 MPa , 0.7 MPa and 1.2 MPa, respectively. So, the fracture strength of the HAp pellets increases with increasing *s:l* ratio This is an expected result as the porosity decreases with increasing the *s:l* ratio of the initial presets produced by mixing PoP and water leading to gypsum. At the two extremes, as reported earlier, (Table 4.1) a minimal *s:l* ratio of 1.33 corresponds to 73.1 vol. % porosity for HAp structures, while the maximum *s:l* of 3.33 leads to products with 61.1 vol %.When the potential ultimate use of the HAp pellets is considered, it is worth to remember that a representative tensile strength value for the porous (cancellous) bone is around 3 MPa [8]**.** In this current study, the most densely packed HAp pellet exhibited a tensile strength of 1.2 MPa, which is nearly 1/3 of the strength values of the bone. The polymer coating, in fact, was mainly performed for this reason; to improve the mechanical properties of the cement-type HAp product. Another reason was related with type of the polymer that has been chosen. The PCL was selected due to its well accepted biocompatibility.

In order to evaluate the possible improvement with polymer coating, HAp pellets (products of *s:l* ratio of 1.33) was coated with PCL as outlined by the experimental protocol in Materials and Methods chapter. The fracture strength value of these PCL-coated HAp pellet is also shown in Table 5.1. The average fracture strength

of the PCL-coated samples increased to 0.6 MPa from an initial value of 0.3 MPa. Meanwhile, some control samples were also prepared and tested to see sole effect of the presence of PCL in coating solution (chloroform based) on the fracture strength of the bulk HAp pellets. The control samples were simply immersed in chloroform solution without PCL addition and fracture strengths were determined. For this particular set, no difference in mechanical properties was observed between the bare HAp and chloroform-immersed HAp pellets, suggesting that increase in the strength is due to the presence of polymer (PCL) itself.

Additionally, a comparison chart for the mechanical properties of the PCL-coated and uncoated HAp structure is provided in Figure 5.3. It is clear that the fracture strength increases from 0.3 MPa to 1.2 MPa with increasing *s:l* ratio accompanied by a decrease in porosity. This chart also shows that the strength doubles, from 0.3 MPa to 0.6 MPa, in the presence of the PCL-coating for the HAp pellets with *s:l* ratio of 1.33. Similar results on improvement of the strength values of porous HAp scafffolds have been reported by some researchers. Zhao et. al. [33] showed that for a porous HAp scaffold, which was also immersed in 10 wt% PCL-chloroform solution, compressive strength (0.5 ± 0.09 MPa) increased 2 times compared to the compressive strength of the uncoated samples (0.27 ± 0.04 MPa). They also address that PCL coating covers the porous surfaces on the HAp pellet; therefore, PCL coating has a positive effect in reinforcing and toughening of HAp/PCL composites. Nalla et. al**.** [41] suggested that the mechanical improvement achieved by the coating is similar to the crack bridging mechanism due to the collagen fibrils in the bone acting as an operational toughening mechanism in the bone.

Table 5.1 Fracture strength of the bulk HAp samples produced from gypsum pellets under hydrothermal-like conditions for 6 h and HAp/PCL composite samples dipped 5 times into PCL-chloroform solution. Fracture strength analyses were conducted using diametrical compression testing method.

Solid to Liquid Ratio (*s:l*)	**Fracture Strength (*MPa*)**
1.33	0.3 ± 0.05
1.67	0.5 ± 0.07
2.22	0.7 ± 0.07
3.33	1.2 ± 0.11
1.33 PCL-coated	0.6 ± 0.05

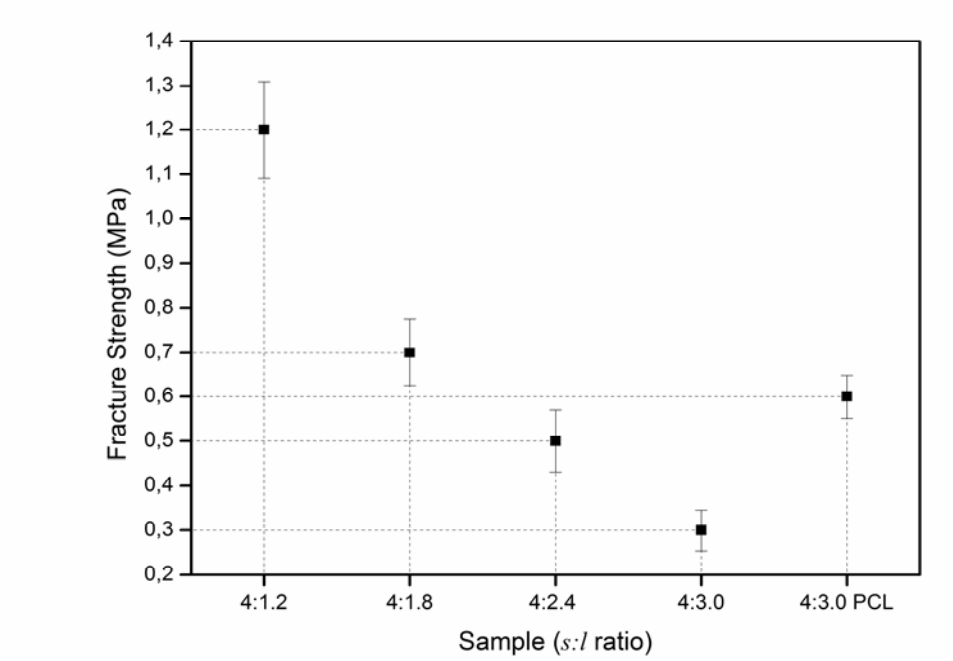

Figure 5.3 Fracture strengths of the HAp samples converted from gypsum pellets having different *s:l* ratios (shown in x-axis of the graph) by 1 M of $(NH_4)_2HPO_4$ solution under hydrothermal-like conditions and the HAp/PCL composite having a HAp phase with a *s:l* ratio of 1.33 in addition to 5-layered PCL coating. As the *s:l* ratio decreases, the fracture strength decreases. Additionally, fracture strength of the PCL-coated sample (abbreviated as *1.33 PCL-coated*) is doubled compared to the uncoated sample.

In order to verify and ensure that PCL was coated to the HAp pellets, heat treatment experiments and SEM studies are performed on the PCL-coated bulk HAp pellets. In the heat treatment experiments, the PCL-coated sample was weighed and then, put in an open air furnace operating at 200 °C for 1 day in order to burn-out the polymeric component. After heat treatment operation, the sample was removed from the furnace and weighed again to observe mass change on the pellet. The pre-heat treated mass was 1.02 g and the post-heat treated mass was 0.92 g. The observed loss in the total mass of the pellet is 0.1 g. The loss in total mass shows that the coating was removed by heat treatment of the PCL-coated sample at 200 °C for 1 day. Additionally, the optical image of the pre- and post-heat treated samples shown in Figure 5.4 illustrates the visible change by the heat treatment process. After the heat treatment operation, the sample color changed from white to brown and in addition to the total mass change; color change is due to burning of carbon species also prove the success for the PCL-coating process.

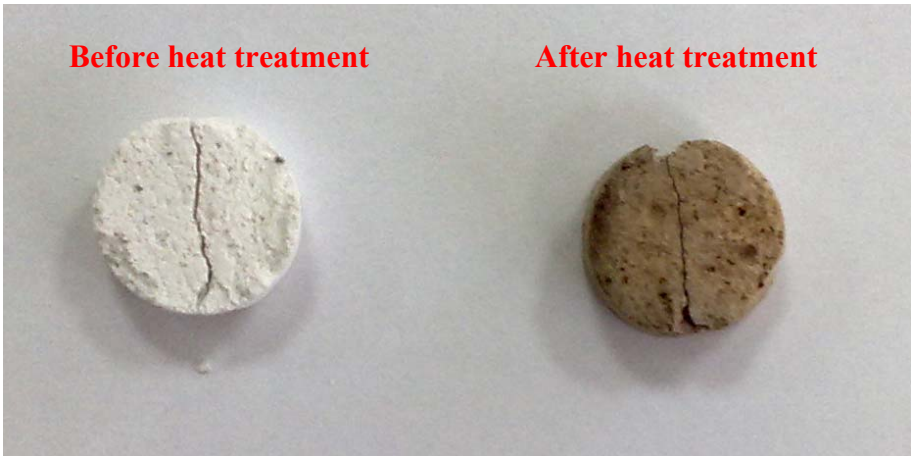

Figure 5.4 Optical images of the PCL-coated HAp pellets before (left) and after (right) the heat treatment process at 200 °C. Color and mass change was observed on the heat treated sample.

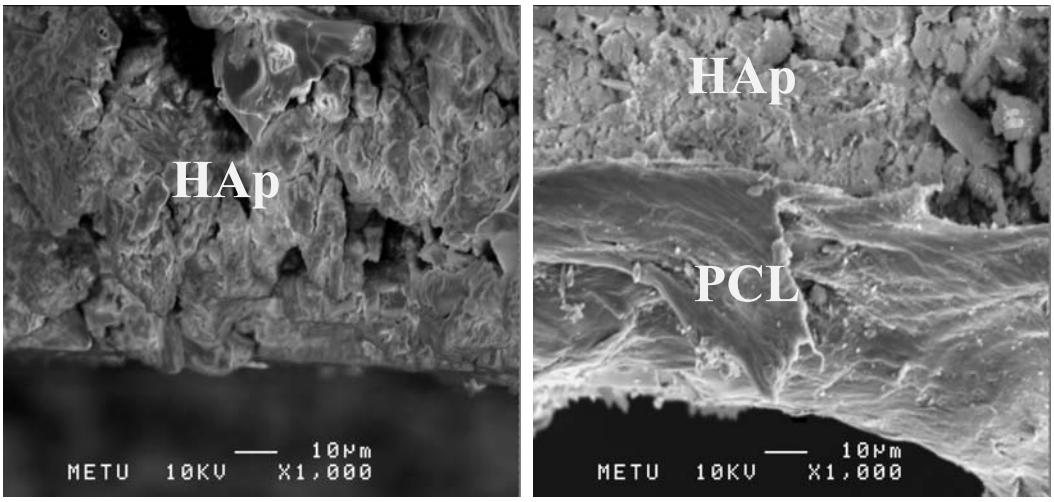

Figure 5.5 SEM micrographs of the uncoated (left) and PCL-coated (right) bulk HAp samples. The HAp and PCL regions are shown in the figure.

Meanwhile, Figure 5.5 shows the SEM micrographs on the PCL-coated and uncoated bulk HAp samples. According to this figure, the thickness of the PCL coating on the HAp surface was measured approximately as 50-60 μm. Additionally; PCL was not infiltrated into the porous network of HAp due to the intrinsic porosity of the HAp network inherited from the densely packed gypsum network shown in Figure 3.9. The SEM micrographs are also clean illustrations of the PCL-coating, most likely filling and healing the cracks on the surface of HAp thereby causing an improvement in strength values. The PCL-coated layer and its structure were also observed in the previous study of Jun et. al. [42] again reporting enhancement in mechanical properties for polymer coated calcium phosphate structures.

CHAPTER 6

CONCLUSIONS

Hydroxyapatite (HAp) formation in powder and bulk form from commercial grade calcium sulfate (plaster of paris, PoP) and its hydration product, gypsum under hydrothermal-like (120 °C and 2 ± 0.2 atm) and ambient conditions (1 atm with varying temperatures) was achieved. Physical, chemical and morphological analyses were performed on starting materials, i.e. PoP and gypsum. In addition phase and morphological studies were conducted on the conversion products, i.e. HAp. Finally, heat treatment studies and mechanical testing by diametrical compression method were performed on selected HAp samples. General findings of the present study can be summarized as the followings:

(i) Properties of PoP and its hydration product, gypsum:

The analyses of starting materials mainly focused on the commercial grade PoP powders. In addition to physical, chemical and morphological studies of PoP, conversion kinetics of PoP to gypsum conversion was also investigated.

As a starting material, commercial grade PoP powders, in general, had a particle size of 54.7 ± 3 μm. with prismatic and equiaxed shaped morphology. It has been found that this type of morphology is similar to α-polymorph of the calcium sulfate. The PoP powders were not pure; therefore additional purification steps should be applied. One of these purification steps may be heat treatment of the PoP powders before conversion reaction to burn or decompose the impurities present in the powders.

Investigation of the conversion (hydration) reaction of PoP powders to bulk gypsum showed that PoP powders are mostly converted to gypsum; however, complete conversion of PoP to gypsum was not always possible. Due to the impure nature of the starting materials, the morphology of the bulk gypsum samples was divided into three distinct parts: calcium sulfate region, perlite (a type of alumina-silicate volcanic glass with elemental silicon) region and porosity created by air bubbles. The hydrated calcium sulfate region had a needle-like morphology and the prismatic morphology of the PoP powders observed.

(ii) Conversion of calcium sulfates to HAp and HAp properties:

The analyses of the conversion products were conducted in two different parts. The first part was the investigation of the conversion products formed under ambient conditions. In this part, the pressure was 1 atm, and the temperature was changed from 25 °C to 90 °C. The reaction times were set from 2 h to 21 days for 25 °C and 2 h to 6 h for other temperatures. At 25 °C, the reactants were mostly converted into brushite after 7 days, and a small amount of HAp was observed. These phases were evolved up to 21 days and they did not decompose into any other calcium phosphate phase and they can be considered as stable. At 50 °C, HAp was not obtained, even for the 6 h-reacted samples. Prolonged reaction times should be observed to investigate other calcium phosphate phases formed at 50 °C. At 90 °C, HAp was observed after 2 h reaction.

The second part was the examination of the conversion products produced under hydrothermal-like conditions (120 °C and 2 ± 0.2 atm). It was observed that PoP powders could completely transform into HAp in 30 min. The hydrated PoP powders, gypsum can also be converted into HAp. However, it was not as crystalline as the HAp converted from PoP powders. Additionally, the morphological analysis has showed that HAp was crystallized on the spherical particles. Nevertheless, it was impossible to analyze the chemical composition for the core of the spherical particles.

Additionally, conversion reaction from bulk gypsum to HAp was also investigated. The conversion was achieved at 2 h; however, in order to obtain more crystalline

structure, all samples were reacted for 6 h. Although the samples are reacted for 6 h, the crystalline structure similar to the reaction with PoP powders was not accomplished. The morphological analyses showed that the needle-like structure of gypsum was disappeared and a different type of needle-like structure formed. This new phase was observed as HAp. The perlite phase and the porosities created by the air bubbles were also observed after conversion to HAp.

(ii) Additional characterization of HAp:

Additional studies were conducted to examine the thermal stability of the HAp powders and to investigate mechanical properties of pure and polycaprolactone (PCL) coated bulk HAp pellets.

In order to determine the exact chemical identity of the HAp phase, heat treatment examinations were performed on 30 min-reacted and 6 h-reacted HAp powder samples converted under hydrothermal-like conditions. The main idea to choose two distinct samples was the considerations of the product stability due to changing reaction time. 6 h-reacted samples was thought to be more stable than 30 min-reacted samples. Both samples were stable up to 600 °C and above 600 °C; they both were converted into β-tricalcium phosphate (β-TCP). In this study, the maximum heat treatment temperature was 1200 °C, and therefore; β-TCP phase was stable up to that temperature.

The mechanical tests were performed on PCL-coated and uncoated bulk HAp samples by using diametrical compression testing method. Bulk HAp pellets were prepared from PoP mixed with water in various solid to liquid (*s:l*) ratios. The measurements showed that the fracture strength of the bulk HAp pellets could be increased after the coating procedure the fracture strength of the samples was doubled.

In summary, calcium sulfate is a cheap and abundant calcium source, and it can be converted to HAp using appropriate phosphate source, such as $(NH_4)_2HPO_4$. The conversion process is easy and can be completed in 30 min. using the hydrothermal-like synthesis method proposed in this thesis. This method allows

production of HAp in powder form as well as in irregular or shaped bulk forms. This method and the experimental approach of the present work can be also employed easily for mass production of such bioceramics in industrial scale. Moreover, the conversion product, HAp is stable up to 600 °C. This shows that the product is calcium-deficient. Calcium-deficiency for HAp is a desired property in biomedical/implant applications, as the inorganic phase of the natural bone is calcium-deficient. Additionally, the bulk forms of HAp exhibit moderate mechanical strength and their strength can be further improved by polymeric coatings.

REFERENCES

1. Suchanek, W. and Yoshimura, M., *Processing and properties of hydroxyapatite-based biomaterials for use as hard tissue replacement implants.* Journal of Materials Research, 1998. **13**(1): p. 94-117.

2. Weiner, S. and Wagner, H.D., *The Material Bone: Structure-Mechanical Function Relations.* Annual Review of Materials Research, 1998. **28**: p. 271-298.

3. LeGeros, R.Z., *Biological and Synthetic Apatites*, in *Hydroxyapatite and Related Materials*, P.W. Brown and B. Constantz, Editors. 1994, CRC Press: Boca Raton, Florida.

4. Vallet-Regi, M. and Gonzales-Calbet, J.M., *Calcium phosphates as substitution of bone tissues.* Progress in Solid State Chemistry, 2004. **32**(1-2): p. 1-31.

5. Wikipedia, *Bone*, http://en.wikipedia.org/wiki/Bone, last visited on August 15th 2010.

6. Stanford, C.M., et al., *Rapidly forming apatitic mineral in an osteoblastic cell line.* Journal of Biological Chemistry, 1995. **270**(16): p. 9420-9428.

7. Hench, L.L., *Biomaterials.* Science, 1980. **208**: p. 826-831.

8. Moore, W.R., Graves, S.E., and Bain, G.I., *Synthetic bone graft substitutes.* Australian and New Zeland Journal of Surgery, 2001. **71**(6): p. 354-361.

9. Dorozhkin, S.V., *Calcium orthophosphate-based biocomposites and hybrid biomaterials.* Journal of Materials Science: Materials in Medicine, 2009. **44**(9): p. 2343-2387.

10. Chevalier, J. and Gremillard, L., *Ceramics for medical applications: A picture for the next 20 years.* Journal of the European Ceramic Society, 2009. **29**(7): p. 1245-1255.

11. Navarro, M., et al., *Biomaterials in orthopaedics.* Journal of The Royal Society, Interface, 2008. **5**(27): p. 1137-1158.

12. Dupuy, J.C., *Bioceramics: a precious asset for medicine*, http://www.cerameurop.com/spip.php?article309, last visited on August 17th 2010.

13. Hench, L.L. and Andersson, Ö., *Bioactive glasses*, in *An Introduction to Bioceramics*, L.L. Hench and J. Wilson, Editors. 1993, World Scientific Publishing: River Edge, NJ. p. 41-62.

14. Kokubo, T., *A/W Glass-Ceramic: Processing and Properties*, in *An Introduction to Bioceramics*, L.L. Hench and J. Wilson, Editors. 1993, World Scientific Publishing: River Edge, NJ. p. 75-88.

15. Ramakrishna, S., et al., *Biomedical applications of polymer-composite materials: a review.* Composites Science and Technology, 2001. **61**(9): p. 1189-1224.

16. Laurencin, C.T. and Khan, Y., *Bone Graft Substitute Materials*, http://emedicine.medscape.com/article/1230616-overview, last visited on August 17th 2010.

17. Yoshimura, M. and Suda, H., *Hydrothermal Processing of Hydroxyapatite: Past, Present and Future*, in *Hydroxyapatite and Related Materials*, P.W. Brown and B. Constantz, Editors. 1994, CRC Press: Boca Raton, FL. p. 45-72.

18. de Groot, K., et al., *Chemistry of Calcium Phosphate Bioceramics*, in *CRC Handbook of Bioactive Ceramics*, T. Yamamuro, L.L. Hench, and J. Wilson, Editors. 1990, CRC Press: Boca Raton, FL. p. 3-15.

19. LeGeros, R.Z. and LeGeros, J.P., *Dense Hydroxpapatie*, in *An Introduction to Bioceramics*, L.L. Hench and J. Wilson, Editors. 1993, World Scientific Publishing: River Edge, NJ. p. 139-180.

20. Roy, D.M. and Linnehan, S.K., *Hydroxyapatite formed from coral skeletal carbonate by hydrothermal exchange.* Nature, 1974. **247**: p. 220-222.

21. Shors, E.C. and Holmes, R.E., *Porous Hydroxyapatite*, in *An Introduction to Bioceramics*, L.L. Hench and J. Wilson, Editors. 1993, World Scientific Publishing: River Edge, NJ. p. 181-198.

22. Sopyan, I., et al., *Porous hydroxyapatite for artificial bone applications.* Science and Technology of Advanced Materials, 2007. **8**(116): p. 116-123.

23. Zhao, J., et al., *The influence of polymer concentrations on the structure and mechanical properties of porous polycaprolactone-coated hydroxyapatite scaffolds.* Applied Surface Science, 2010. **256**(14): p. 4586-4590.

24. Furuta, S., Katsuki, H., and Komarneni, S., *Porous hydroxyapatite monoliths from gypsum waste.* Journal of Materials Chemistry, 1998. **8**(12): p. 2803-2806.

25. Furuta, S., Katsuki, H., and Komarneni, S., *Removal of lead ions using porous hydroxyapatite monoliths synthesized from gypsum waste.* Journal of the Ceramic Society of Japan, 2000. **108**(3): p. 315-317.

26. Katsuki, H., Furuta, S., and Komarneni, S., *Microwave- versus conventional-hydrothermal synthesis of hydroxyapatite crystals from gypsum.* Journal of American Ceramic Society, 1999. **82**(8): p. 2257-2259.

27. Lowmunkong, R., et al., *Fabrication of freeform bone-filling calcium phosphate ceramics by gypsum 3D printing method.* Journal of Biomedical Materials Research Part B: Applied Biomaterials, 2008. **90B**(2): p. 531-539.

28. Lowmunkong, R., et al., *Transformation of 3DP gypsum model to HA by treating in ammonium phosphate solution.* Journal of Biomedical Materials Research Part B: Applied Biomaterials, 2006. **80**(2): p. 386-393.

29. Peltier, L.F., et al., *The use of plaster of paris to fill defects in bone.* Annual Surgery, 1957. **146**(1): p. 61-69.

30. Thomas, M.V. and Puleo, D.A., *Calcium Sulfate: Properties and Clinical Applications.* Journal of Biomedical Materials Research Part B: Applied Biomaterials, 2008. **88**(2): p. 597-610.

31. Khan, S.N., Tomin, E., and Lane, J.M., *Clinical applications of bone graft substitutes.* Orthopedic Clinics of North America, 2000. **31**(3): p. 389-398.

32. Wikipedia, *Polycaprolactone*, http://en.wikipedia.org/wiki/Polycaprolactone, last visited on August 8th 2010.

33. Zhao, J., et al., *Preparation of bioactive porous HA/PCL composite scaffolds.* Applied Surface Science, 2008. **255**(5): p. 2942-2946.

34. Durucan, C. and Brown, P.W., *Biodegradable hydroxyapatite-polymer composites.* Advanced Engineering Materials, 2001. **3**(4): p. 227-231.

35. Thomas, M.B., et al., *Dense hydroxyapatite: Fatigue and fracture strength after various treatments, from diametral tests.* Journal of Materials Science, 1980. **15**(4): p. 891-894.

36. ASTM, *Standard Test Method for Tensile Strength of Concrete Surfaces and the Bond Strength or Tensile Strength of Concrete Repair and Overlay Materials by Direct Tension (Pull-off Method)*. 2004, ASTM International.

37. Kanos, A., Giannakopoulos, A.E., and Perdikaris, P.C., *Effect of concrete splitting tensile strength and modulus of elasticity*, in *Measuring, Monitoring and Modeling Concrete Properties*, M.S. Konsta-Gdoutos, Editor. 2006, Springer: The Netherlands. p. 239-246.

38. Doğan, H., Koral, M., and Kocakuşak, S., *Acid leaching of Turkish celestite concentrate.* Hydrometallurgy, 2004. **71**(3-4): p. 379-383.

39. Playa, E. and Rosell, L., *The celestite problem in gypsum Sr geochemistry: An evaluation of purifying methods of gypsiferous samples.* Chemical Geology, 2005. **221**(1-2): p. 102-116.

40. Kreidler, E.R. and Hummel, F.A., *Phase relationships in the system SrO-P_2O_5 and the influence of water vapor on the formation of $Sr_4P_2O_9$.* Inorganic Chemistry, 1967. **6**(5): p. 884-891.

41. Nalla, R.K., Kinley, J.H., and Ritchie, R.O., *Mechanistic fracture criteria for the failure of human cortical bone.* Nature Materials, 2003. **2**(3): p. 164-168.

42. Jun, I.-K., et al., *Novel fabrication of a polymer scaffold with a dense bioactive ceramic coating layer.* Journal of Materials Science: Materials in Medicine, 2007. **18**(8): p. 1537-1542.